Power diagrams and interaction processes for unions of discs

Møller, Jesper; Helisova, Katarina

Publication date:
2007

Document Version
Publisher's PDF, also known as Version of record

AALBORG UNIVERSITY

Power diagrams and interaction processes for unions of discs

by

Jesper Møller and Kateřina Helisová

R-2007-15 July 2007

Department of Mathematical Sciences
Aalborg University
Fredrik Bajers Vej 7 G ▪ DK - 9220 Aalborg Øst ▪ Denmark
Phone: +45 96 35 80 80 ▪ Telefax: +45 98 15 81 29
URL: www.math.auc.dk/research/reports/reports.htm

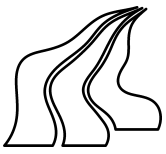

ISSN 1399–2503 ▪ On-line version ISSN 1601–7811

30 July 2007

POWER DIAGRAMS AND INTERACTION PROCESSES FOR UNIONS OF DISCS

JESPER MØLLER,* *Aalborg University*

KATEŘINA HELISOVÁ,** *Charles University in Prague*

Abstract

We study a flexible class of finite disc process models with interaction between the discs. We let $\mathcal{U}$ denote the random set given by the union of discs, and use for the disc process an exponential family density with the canonical sufficient statistic only depending on geometric properties of $\mathcal{U}$ such as the area, perimeter, Euler-Poincaré characteristic, and number of holes. This includes the quarmass-interaction process and the continuum random cluster model as special cases. Viewing our model as a connected component Markov point process, and thereby establish local and spatial Markov properties, becomes useful for handling the problem of edge effects when only $\mathcal{U}$ is observed within a bounded observation window. The power tessellation and its dual graph become major tools when establishing inclusion-exclusion formulae, formulae for computing geometric characteristics of $\mathcal{U}$, and stability properties of the underlying disc process density. Algorithms for constructing the power tessellation of $\mathcal{U}$ and for simulating the disc process are discussed, and the software is made public available.

Keywords: Area-interaction process, Boolean model; disc process; exponential family; germ-grain model; local computations; local stability; Markov properties; inclusion-exclusion formulae; interaction; point process; power tessellation; simulation; quarmass-interaction process; random closed set; Ruelle stability

AMS 2000 Subject Classification: Primary 60D05;60G55;60K35;62M30

Secondary 68U20

* Postal address: Department of Mathematical Sciences, Aalborg University Fredrik Bajers Vej 7G, DK-9220 Aalborg, Denmark. Email address: jm@math.auc.dk

** Postal address: Department of Probability and Mathematical Statistics, Charles University in Prague, Sokolovská 83, 18675 Praha 8, Czech Republic. Email address: helisova@karlin.mff.cuni.cz

1. Introduction

This paper concerns probabilistic results of statistical relevance for planar random set models given by a finite union of discs $\mathcal{U} = \mathcal{U}_{\mathbf{X}}$, where $\mathbf{X}$ denotes the corresponding finite process of discs. We distinguish between the case where we can observe the discs in $\mathbf{X}$ and the random set case where only (or at most) $\mathcal{U}$ is observed. The latter case occur frequently in applications and will be of main interest to us.

Our random closed set $\mathcal{U}$ is a particular example of a germ-grain model [17], with the grains being discs. It is well-known that any random closed set whose realizations are locally finite unions of compact convex sets is a germ-grain model with convex and compact grains [41, 42]. However, in order to make statistical inference, one needs to restrict attention to a much smaller class of models such as a random-disc process model, and indeed random-disc Boolean models play the main role in practice, see [40] and the references therein. The Boolean model is in an abstract setting given by a Poisson process of compact sets (the grains) with no interaction between the grains. Many authors (e.g. [2, 8, 9, 16, 19, 40]) have mentioned the need of developing flexible germ-grain models with interaction between the grains.

We study a particular class of models for interaction among the discs, specified by a point process density for $\mathbf{X}$ with respect to a reference Poisson process of discs. The density is assumed to be of exponential family form, with the canonical sufficient statistic $T(\mathbf{X}) = T(\mathcal{U})$ only depending on $\mathbf{X}$ through $\mathcal{U}$, where $T(\mathcal{U})$ is specified in terms of geometric characteristics for the connected components of $\mathcal{U}$, for example, the area $A(\mathcal{U})$, the perimeter $L(\mathcal{U})$, the number of holes $N_{\mathrm{h}}(\mathcal{U})$, and the number of connected components $N_{\mathrm{cc}}(\mathcal{U})$. Further geometric characteristics are specified in Section 4.1 in terms of the power tessellation (e.g. [1]), which provides a subdivision of $\mathcal{U}$ (see Figure 2 in Section 3). An important special case of our models is the quarmass-interaction process, first introduced in Kendall, van Lieshout and Baddeley [19], where $T(\mathcal{U}) = (A(\mathcal{U}), L(\mathcal{U}), \chi(\mathcal{U}))$ and $\chi(\mathcal{U}) = N_{\mathrm{cc}}(\mathcal{U}) - N_{\mathrm{h}}(\mathcal{U})$ is the Euler-Poincaré characteristic (quarmass-integrals in $\mathbb{R}^2$ are linear combinations of A, L, χ). Another special case is the continuum random cluster model [15, 23, 28], where $T(\mathcal{U}) = N_{\mathrm{cc}}(\mathcal{U})$.

We show that the power tessellation and its dual graph are extremely useful when establishing

(i) inclusion-exclusion formulae for $T(\mathcal{U})$;

(ii) formulae for computing geometric characteristics of $\mathcal{U}$;

(iii) Ruelle and local stability of the density of $\mathbf{X}$, and thereby convergence properties of MCMC algorithms for simulating $\mathbf{X}$.

Among other things we demonstrate that a main geometric result in [19] related to the issue of Ruelle stability is easily derived by means of the power tessellation and its dual graph. Furthermore, as explained in Section 4.5, it becomes useful to view our models as connected component Markov point processes [2, 4, 7, 30] in a similar way as the Markov connected component fields studied in [32]. In particular, we establish

(iv) local and spatial Markov properties of $\mathbf{X}$, which become useful for handling the problem of edge effects when only $\mathcal{U}$ is observed within a bounded observation window.

The paper is organized as follows. Section 2 specifies our notation and assumptions, and discusses a general position property of the discs in $\mathbf{X}$. Section 3 defines and studies the power tessellation of a union of discs in general position. The main section, Section 4, studies exponential family properties and the above-mentioned issues (i)-(iv). Also various examples of simulated realizations of our models are shown in Section 4. Section 5 discusses extensions of our work and some open problems. Finally, most algorithmic details are deferred to Appendices A-B.

A substantial part of this work has been the developments of codes in `C` and `R` for constructing power tessellations and making simulations of our models. The codes are available at `www.math.aau.dk/~jm/Codes.union.of.discs`.

2. Preliminaries

2.1. Setup

Throughout this paper we use the following notation and make the following assumptions.

By a disc we mean more precisely a two-dimensional closed disc $b = \{y \in \mathbb{R}^2 : \|y - z\| \leq r\}$ with centre $z \in \mathbb{R}^2$ and positive radius $r > 0$, where $\|\cdot\|$ denotes usual

Euclidean distance. We identify b with the point $x = (z, r)$ in $\mathbb{R}^2 \times (0, \infty)$, and write $b = b(x) = b(z, r)$. Similarly, we identify point processes of discs $b_i = b(z_i, r_i)$ with point processes on $\mathbb{R}^2 \times (0, \infty)$.

The reference point process will be a Poisson process $\mathbf{\Psi}$ of discs; thus the random set given by the union of discs in $\mathbf{\Psi}$ is a Boolean model (e.g. [27]). Specifically, $\mathbf{\Psi}$ is assumed to be a Poisson point process on $\mathbb{R}^2 \times (0, \infty)$, with an intensity measure of the form $\rho(z)\,\mathrm{d}z\,Q(\mathrm{d}r)$, where $\mathrm{d}z$ is Lebesgue measure on $\mathbb{R}^2$ and Q is an arbitrary probability measure on $(0, \infty)$. In other words, the point process $\mathbf{\Phi}$ of centres of discs given by $\mathbf{\Psi}$ is a Poisson process with intensity function ρ on $\mathbb{R}^2$, the radii of these discs are mutually independent and identically distributed with distribution Q, and $\mathbf{\Phi}$ is independent of the radii. An example of a simulation from such a process is shown in Figure 1. The concrete specification of ρ and Q is not important for most results in this paper, but the specification is of course crucial for statistical inference, see [31]. Local integrability of ρ is assumed to ensure that with probability one, $\mathbf{\Phi} \cap S$ is finite for any bounded region $S \subset \mathbb{R}^2$. Since we can view the radii as marks associated to the points given by the centres of the discs, we refer to Q as the *mark distribution*. In the special case where Q is degenerate at $R > 0$, we can consider R as a parameter and identify $\mathbf{\Psi}$ with $\mathbf{\Phi}$.

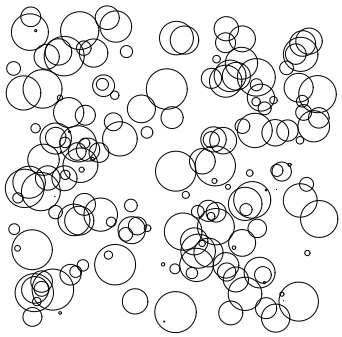

FIGURE 1: A realization of a reference Poisson process with Q the uniform distribution on the interval $[0, 2]$, $\rho(u) = 0.2$ on a rectangular region $S = [0, 30] \times [0, 30]$, and $\rho(u) = 0$ outside S.

In the sequel, S denotes a given bounded planar region such that $\int_S \rho(z)\,\mathrm{d}z > 0$.

The object of primary interest is the random closed set

$$\mathcal{U}_{\mathbf{X}} = \cup_{x \in \mathbf{X}} b(x)$$

where $\mathbf{X}$ is a finite point process defined on $S \times (0, \infty)$. If $\mathbf{X} = \emptyset$ is the empty configuration, we let $\mathcal{U}_{\mathbf{X}} = \emptyset$ be the empty set. Note that the centres of the discs are contained in S but the discs may extend outside S. We assume that $\mathbf{X}$ is absolutely continuous with respect to the reference Poisson process $\mathbf{\Psi}$, and denote the density by $f(\mathbf{x})$ for finite configurations $\mathbf{x} = \{x_1, \ldots, x_n\}$ with $x_i = (z_i, r_i) \in S \times (0, \infty)$ and $0 \leq n < \infty$ (if $n = 0$ then $\mathbf{x}$ is the empty configuration).

We focus on the case where the density is of the exponential family form

$$f_\theta(\mathbf{x}) = \exp\left(\theta \cdot T(\mathcal{U}_{\mathbf{x}})\right) / c_\theta \tag{1}$$

where θ is a real parameter vector, $\cdot$ denotes the usual inner product, $T(\mathcal{U})$ is a statistic of the same dimension as θ, and c_θ is a normalizing constant depending on θ (and of course also on (T, ρ, Q)). Note that $f_\theta(\mathbf{x}) > 0$ for all $\mathbf{x}$. Further details on the choice of T and the parameter space for θ are given in Section 4. Note that (1) is also the density of the random set $\mathcal{U}_{\mathbf{X}}$ with respect to the reference Boolean model, and

$$\begin{aligned} c_\theta = &\exp\left(-\int_S \rho(z)\,\mathrm{d}z\right) \times \Bigg[\exp(\theta \cdot T(\emptyset)) + \sum_{n=1}^{\infty} \int_S \int_0^\infty \cdots \int_S \int_0^\infty \\ &\exp\left(\theta \cdot T\left(\mathcal{U}_{\{(z_1,r_1),\ldots,(z_n,r_n)\}}\right)\right) \prod_1^n \rho(z_i)\,\mathrm{d}z_1\, Q(\mathrm{d}r_1) \cdots \mathrm{d}z_n\, Q(\mathrm{d}r_n)\Bigg] \end{aligned} \tag{2}$$

is in general not expressible on closed form (unless $\theta \neq 0$).

As noticed in Section 1, a quarmass-interaction process is obtained by taking $T(\mathcal{U}) = (A(\mathcal{U}), L(\mathcal{U}), \chi(\mathcal{U}))$, where $A(\mathcal{U})$ is the area, $L(\mathcal{U})$ the perimeter and $\chi(\mathcal{U})$ the Euler-Poincaré characteristic of $\mathcal{U}$. We consider here the so-called additive extension of the Euler-Poincaré characteristic, which is also of primary interest in [19], i.e.

$$\chi(\mathcal{U}) = N_{\mathrm{cc}}(\mathcal{U}) - N_{\mathrm{h}}(\mathcal{U}) \tag{3}$$

where $N_{\mathrm{cc}}(\mathcal{U})$ is the number of connected components of $\mathcal{U}$ and $N_{\mathrm{h}}(\mathcal{U})$ is the number of holes of $\mathcal{U}$. The special case where Q is degenerate and $T(\mathcal{U}) = A(\mathcal{U})$ is known as the area-interaction point process, Widom-Rowlinson model or penetrable spheres model, see e.g. [3, 15, 19, 43].

2.2. General position of discs

It becomes essential in this paper that with probability one, the discs defined by $\mathbf{\Psi}$ are in general position in the following sense. Identify $\mathbb{R}^2$ with the hyperplane of $\mathbb{R}^3$ spanned by the first two coordinate axes. For each disc $b(z,r)$, define the *ghost sphere* $s(z,r) = \{y \in \mathbb{R}^3 : \|y - z\| = r\}$, i.e. the hypersphere in $\mathbb{R}^3$ with centre z and radius r. A configuration of discs is said to be in *general position* if the intersection of any $k+1$ corresponding ghost spheres is either empty or a sphere of dimension $2-k$, where $k = 1, 2, \ldots$. Note that the intersection is assumed to be empty if $k > 2$, and a sphere of dimension 0 is assumed to consists of two points. The upper left panel in Figure 2 shows a configuration of discs in general position; we shall use this as a running example to illustrate forthcoming definitions.

Lemma 1. *For almost all realizations of $\mathbf{\Psi} = \{x_1, x_2, \ldots\}$, the discs $b_1 = b(x_1),\ b_2 = b(x_2),\ \ldots$ are in general position.*

Proof. By Campbell's theorem (see e.g. [40]), the mean number of sets of $k+1$ ghost spheres whose intersection is neither empty nor of dimension $2-k$ is given by

$$\int_{\mathbb{R}^2} \int_0^\infty \cdots \int_{\mathbb{R}^2} \int_0^\infty \mathbf{1}\left[\cap_0^k s_i \neq \emptyset,\, \dim\left(\cap_0^k s_i\right) \neq 2-k\right] \frac{\prod_0^k \rho(z_i)}{(k+1)!}\, \mathrm{d}z_0\, Q(\mathrm{d}r_0) \cdots \mathrm{d}z_k\, Q(\mathrm{d}r_k)$$

where $\mathbf{1}[\cdot]$ is the indicator function and $s_i = s(z_i, r_i)$. This integral is zero, since for any fixed values of $r_0 > 0, \ldots, r_k > 0$, the indicator function is zero for Lebesgue almost all $(z_0, \ldots, z_k) \in \mathbb{R}^{2(k+1)}$.

All point process models for discs considered in this paper have discs in general position: by Lemma 1, the discs in $\mathbf{X}$ with density (1) are in general position almost surely.

3. Power tessellation of a union of discs

This section defines and studies the power tessellation of a union of discs $\mathcal{U} = \cup_{i \in I} b_i$. We assume that the discs $b_i,\ i \in I$ satisfy the general position assumption (henceforth GPA).

3.1. Basic definitions

In this section, there is no need for assuming that the index set I is finite, though this will be the case in subsequent sections.

For each disc b_i ($i \in I$) with ghost sphere s_i, let $s_i^+ = \{(y_1, y_2, y_3) \in s_i : y_3 \geq 0\}$ denote the corresponding upper hypersphere, and for $u \in b_i$, let $y_i(u)$ denote the unique point on s_i^+ those orthogonal projection on $\mathbb{R}^2$ is u. The subset of s_i^+ consisting of those points "we can see from above" is given by

$$C_i = \{y_i(u) : u \in b_i,\ \|u - y_i(u)\| \geq \|u - y_j(u)\| \text{ whenever } u \in b_j,\ j \in I\},$$

and the GPA implies that the non-empty C_i have disjoint 2-dimensional relative interiors. Thus, as illustrated in the upper right panel in Figure 2, the non-empty C_i form a tessellation (i.e. subdivision) of $\cup_I s_i^+$ corresponding to the 2-dimensional pieces of upper ghost spheres "as seen from above". Projecting this tessellation onto $\mathbb{R}^2$, we obtain a tessellation of $\mathcal{U}$, see the lower left panel in Figure 2. Below we specify this tessellation in detail.

Let $J = \{i \in I : C_i \neq \emptyset\}$. For $i \in I$, define the *power distance* of a point $u \in \mathbb{R}^2$ from $b_i = b(z_i, r_i)$ by $\pi_i(u) = \|u - z_i\|^2 - r_i^2$, and define the *power cell* associated with b_i by

$$V_i = \{u \in \mathbb{R}^2 : \pi_i(u) \leq \pi_j(u) \text{ for all } j \in I\}.$$

For distinct $i, j \in I$, define the closed halfplane $H_{i,j} = \{u \in \mathbb{R}^2 : \pi_i(u) \leq \pi_j(u)\}$. Each V_i is a convex polygon, since it is a finite intersection of closed halfplanes $H_{i,j}$. The power cells have disjoint interiors, and by GPA, each V_i is either empty or of dimension two. Consequently, the non-empty power cells V_i, $i \in J$ constitute a tessellation of $\mathbb{R}^2$ called the *power diagram* (or *Laguerre diagram*), see [1] and the references therein. In the special case where all radii r_i are equal, we have $I = J$ and the power diagram is a Voronoi tessellation (e.g. [29, 35]) where each cell V_i contains z_i in its interior. If the radii are not equal, a power cell V_i may not contain z_i, since $H_{i,j}$ may not contain z_i.

Let B_i denote the orthogonal projection of C_i on $\mathbb{R}^2$. By Pythagoras, for all $u \in b_i$, $\pi_i(u) + \|u - y_i(u)\|^2 = 0$. Consequently, for any $i, j \in I$ and $u \in b_i \cap b_j$,

$$\|u - y_i(u)\| \geq \|u - y_j(u)\| \quad \text{if and only if} \quad \pi_i(u) \leq \pi_j(u).$$

Thus $B_i = V_i \cap b_i$. By GPA and the one-to-one correspondence between B_i and C_i, the collection of sets $B_i,\ i \in J$ constitutes a subdivision of $\mathcal{U}$ into 2-dimensional convex sets with disjoint interiors. We call this the *power tessellation of the union of discs* and denote it by $\mathcal{B}$. Further, if $i \in J$, we call B_i the *power cell restricted to its associated disc* b_i (clearly, $B_i = \emptyset$ if $i \in I \setminus J$). Since V_i may not contain z_i, B_i may not contain z_i; an example of this is shown in the lower left panel in Figure 2. We say that a cell B_i is *isolated* if $B_i = b_i$. This means that any disc $b_j,\ j \in I$, intersecting b_i is contained in b_i; the disc b_i is therefore also said to be a circular clump, see [27] and the references therein.

It is illuminating to consider Figure 2 when making the following definitions. If the intersection $e_{i,j} = B_i \cap B_j$ between two cells of $\mathcal{B}$ is non-empty, then $e_{i,j} = [u_{i,j}, v_{i,j}]$ is a closed line segment, where $u_{i,j}$ and $v_{i,j}$ denote the endpoints, and we call $e_{i,j}$ an *interior edge* of $\mathcal{B}$. The vertices of $\mathcal{B}$ are given by all endpoints of interior edges. A vertex of $\mathcal{B}$ lying on the boundary $\partial\mathcal{U}$ is called a *boundary vertex*, and it is called an *interior vertex* otherwise. Each circular arc on $\mathcal{B}$ defined by two successive boundary vertices is called a *boundary edge* of $\mathcal{B}$. The circle given by the boundary of an isolated cell of $\mathcal{B}$ is also called a boundary edge or sometimes an *isolated boundary edge*. The connected components of $\partial\mathcal{U}$ are closed curves, and each such curve is a union of certain boundary edges which either bound a hole, in which case the curve is called an *inner boundary curve*, or bound a connected component of $\mathcal{U}$, in which case the curve is called an *outer boundary curve*. A generic boundary edge of $\mathcal{B}$ is written as $\lfloor u_i, v_i \rceil$ if $B_i \neq b_i$ (a non-isolated cell), where the index means that u_i and v_i are boundary vertices of B_i, or as ∂b_i if $B_i = b_i$. We order u_i and v_i such that $\lfloor u_i, v_i \rceil$ is the circular arc from u_i to v_i when ∂b_i is considered anti-clockwise.

By GPA, any intersection among four cells of $\mathcal{B}$ is empty, each interior vertex corresponds to a non-empty intersection among three cells of $\mathcal{B}$, and exactly three edges emerge at each vertex. Note that each isolated cell has no vertices and one edge. Each interior edge $e_{i,j}$ is contained in the *bisector (or power line or radical axis)* of b_i and b_j defined by $\partial H_{i,j} = \{u \in \mathbb{R}^d : \pi_i(u) = \pi_j(u)\}$. This is the line perpendicular to the line joining the centres of the two discs, and passing through the point

$$z_{i,j} = \frac{1}{2}\left(z_i + z_j + \frac{r_j^2 - r_i^2}{\|z_i - z_j\|^2}(z_i - z_j)\right).$$

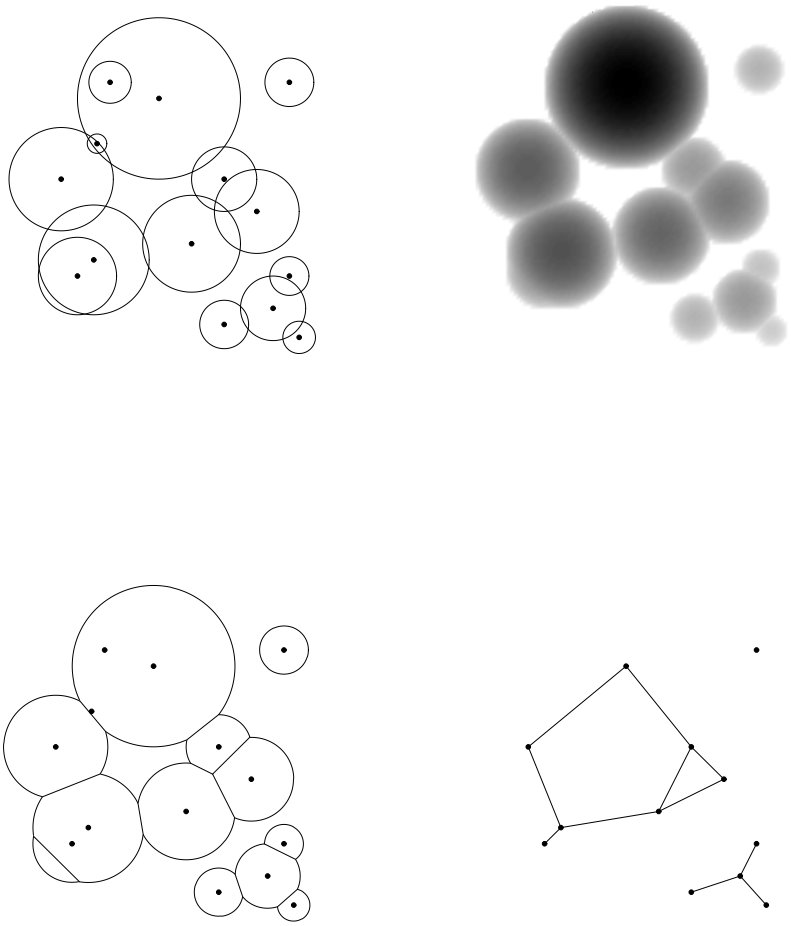

FIGURE 2: Upper left panel: A configuration of discs in general position. Upper right panel: The upper hemispheres as seen from above. Lower left panel: The power tessellation of the union of discs. Lower right panel: The dual graph.

We call $E_{i,j} \equiv \partial H_{i,j} \cap b_i = \partial H_{i,j} \cap b_j$ the *chord* of $b_i \cap b_j$. Obviously, $e_{i,j} \subseteq E_{i,j}$.

The *dual graph* $\mathcal{D}$ to $\mathcal{B}$ has nodes equal to the centres $z_i,\ i \in J$ of discs generating non-empty cells, and each edge of $\mathcal{D}$ is given by two vertices z_i and z_j such that $e_{i,j} \neq \emptyset$. See the lower right panel in Figure 2. Note that there is a one-to-one correspondence

between the edges of $\mathcal{D}$ and the interior edges of $\mathcal{B}$.

3.2. Construction

We construct the power tessellation of a finite union of discs by successively adding the discs one by one, keeping track on old and new edges and whether each disc generates a non-empty cell or not. The updates are local in some sense and used in the "birth-part" of the MCMC algorithm in Section 4.7. For details, see Appendix A.

4. Results for exponential family models

This section studies exponential family models for the point process $\mathbf{X}$ as specified by the density $f(\mathbf{x})$ in (1), assuming that the canonical sufficient statistic $T(\mathcal{U}_{\mathbf{x}})$ is a linear combination of one or more of the geometric characteristics introduced in the following paragraph. We let $\mathrm{supp}(Q)$ denote the support of Q,

$$\Omega = \{(z, r) \in S \times (0, \infty) : \rho(z) > 0, r \in \mathrm{supp}(Q)\}$$

the support of the intensity measure of the reference Poisson process $\mathbf{\Psi}$, and $\mathcal{N}$ the set of all finite subsets $\mathbf{x}$ (also called finite configurations) of Ω so that the discs given by $\mathbf{x}$ are in general position. By Lemma 1, $\mathbf{X} \in \mathcal{N}$ with probability one. For ease of exposition we assume that all realizations of $\mathbf{X}$ are in $\mathcal{N}$, and set $f(\mathbf{x}) = 0$ if $\mathbf{x} \notin \mathcal{N}$.

We let $T(\mathbf{x})$ be given by one or more of the following characteristics of $\mathcal{U} = \mathcal{U}_{\mathbf{x}}$ if $\mathbf{x} \in \mathcal{N}$: the area $A = A(\mathcal{U})$, the perimeter $L = L(\mathcal{U})$, the Euler-Poincaré characteristic $\chi = \chi(\mathcal{U})$, the number of isolated cells $N_{\mathrm{ic}} = N_{\mathrm{ic}}(\mathcal{U})$, the number of connected components $N_{\mathrm{cc}} = N_{\mathrm{cc}}(\mathcal{U})$, the number of holes $N_{\mathrm{h}} = N_{\mathrm{h}}(\mathcal{U})$, the number of boundary edges (including isolated boundary edges) $N_{\mathrm{be}} = N_{\mathrm{be}}(\mathcal{U})$, and the number of boundary vertices $N_{\mathrm{bv}} = N_{\mathrm{bv}}(\mathcal{U})$. In the general case,

$$T = (A, L, \chi, N_{\mathrm{h}}, N_{\mathrm{ic}}, N_{\mathrm{bv}}) \tag{4}$$

with corresponding canonical parameter $\theta = (\theta_1, \ldots, \theta_6)$, and we call then $\mathbf{X}$ the *T-interaction process*. If e.g. $\theta_2 = \ldots = \theta_6 = 0$, we set $T = A$ and refer then to the A-interaction process. Similarly, for the L-interaction process we have $\theta_1 = 0$ and $\theta_3 = \ldots = \theta_6 = 0$, for the (A, L)-interaction process we have $\theta_3 = \ldots = \theta_6 = 0$, and so on. A quarmass-interaction process [19] is the special case $T = (A, L, \chi)$ and

$\theta_4 = \theta_5 = \theta_6 = 0$. Note that (4) specifies $N_{\rm cc} = \chi + N_{\rm h}$ and $N_{\rm be} = N_{\rm ic} + N_{\rm bv}$, cf. Lemma 2 below. Thus a continuum random cluster model [15, 23, 28] is the special case $T = N_{\rm cc}$, $\theta_1 = \theta_2 = \theta_5 = \theta_6 = 0$, and $\theta_3 = \theta_4$.

4.1. Exponential family structure

Let

$$\Theta = \{(\theta_1, \ldots, \theta_6) \in \mathbb{R}^6 : \int \exp\left(\pi\theta_1 r^2 + 2\pi\theta_2 r\right)\, Q(\mathrm{d}r) < \infty\}. \tag{5}$$

Note that $(-\infty, 0]^2 \times \mathbb{R}^4 \subseteq \Theta$, and $\Theta = \mathbb{R}^6$ if $\mathrm{supp}(Q)$ is bounded. The following proposition states that under a weak condition on (S, ρ, Q), the exponential family density has Θ as its full parameter space and T in (4) as its minimal canonical sufficient statistic (for details on exponential family properties, see [5]).

Proposition 1. *Suppose that S contains a set $D = b(u, R_1) \setminus b(u, R_2)$, where $\infty > R_1 > R_2 > 0$, $\rho(z) > 0$ for all $z \in D$, and $Q((0, R_2]) > 0$. Then the point process densities*

$$f_\theta(\mathbf{x}) = \frac{1}{c_\theta} \exp\left(\theta_1 A(\mathcal{U}_\mathbf{x}) + \theta_2 L(\mathcal{U}_\mathbf{x}) + \theta_3 \chi(\mathcal{U}_\mathbf{x}) + \theta_4 N_{\rm h}(\mathcal{U}_\mathbf{x}) + \theta_5 N_{\rm ic}(\mathcal{U}_\mathbf{x}) + \theta_6 N_{\rm bv}(\mathcal{U}_\mathbf{x})\right) \tag{6}$$

with $\mathbf{x} \in \mathcal{N}$ and $\theta = (\theta_1, \ldots, \theta_6) \in \Theta$ constitute a regular exponential family model.

Proof. Recall that an exponential family model is regular if it is full and of minimal form [5]. We verify later in Proposition 6 that f_θ is well-defined if and only if $\theta \in \Theta$, so the model is full. Let $\mathbf{\Psi}_S$ denote the restriction of $\mathbf{\Psi}$ to $S \times (0, \infty)$. Since $\Theta \supseteq (-\infty, 0]^2 \times \mathbb{R}^4$ is of full dimension 6, and since there is a one-to-one linear correspondence between T in (4) and $(A, L, N_{\rm cc}, N_{\rm ic}, N_{\rm bv}, N_{\rm h})$, the model is on minimal form if the statistics A, L, $N_{\rm ic}$, $N_{\rm cc}$, $N_{\rm bv}$, $N_{\rm h}$ are affinely independent with probability one with respect to $\mathbf{\Psi}_S$, see [5]. In other words, the model is on minimal form if for any $(\alpha_0, \ldots, \alpha_6) \in \mathbb{R}^7$, with probability one,

$$\begin{aligned} &\alpha_1 A(\mathcal{U}_{\mathbf{\Psi}_S}) + \alpha_2 L(\mathcal{U}_{\mathbf{\Psi}_S}) + \alpha_3 N_{\rm ic}(\mathcal{U}_{\mathbf{\Psi}_S}) + \alpha_4 N_{\rm cc}(\mathcal{U}_{\mathbf{\Psi}_S}) + \alpha_5 N_{\rm bv}(\mathcal{U}_{\mathbf{\Psi}_S}) + \alpha_6 N_{\rm h}(\mathcal{U}_{\mathbf{\Psi}_S}) \\ =&\alpha_0 \;\Rightarrow\; \alpha_0 = \ldots = \alpha_6 = 0. \end{aligned} \tag{7}$$

We verify this, using the condition on (S, ρ, Q) imposed in the proposition, and considering realizations of Ψ_S as described below, where these realizations consist of

configurations of discs with centres in D and radius $\leq R_2$. For such configurations, given by either one disc, two non-overlapping discs, or two overlapping discs, and if $\alpha_5 = \alpha_6 = 0$, we immediately obtain (7). Extending this to situations where only $\alpha_6 = 0$ and we have three discs with pairwise overlap but no common intersection, we also immediately obtain (7), and the set consisting of such configurations and where $N_h(\mathcal{U}_{\mathbf{\Psi}_S}) = 0$ has a positive probability. The condition on (S, ρ, Q) also allow us with a positive probability to construct a set of realizations of where $N_h(\mathcal{U}_{\mathbf{\Psi}_S}) = 1$, namely by considering sequences of discs which only overlap pairwise and which form a single connected component. Thereby, for any $(\alpha_0, \ldots, \alpha_6) \in \mathbb{R}^7$, with probability one, (7) is seen to hold.

4.2. Interpretation of parameters

This section discusses the meaning of the parameters $\theta_1, \ldots, \theta_6$ in the T-interaction process (6).

We first recall the definition of the *Papangelou conditional intensity* $\lambda(\mathbf{x}, v)$ for a general finite point process $\mathbf{X} \subset S \times (0, \infty)$ with an hereditary density f with respect to the distribution of $\mathbf{\Psi}$ (see [33] and the references therein). For all finite configurations $\mathbf{x} \subset S \times (0, \infty)$ and all discs $v = (z, r) \in S \times (0, \infty) \setminus \mathbf{x}$, the hereditary condition means that $f(\mathbf{x}) > 0$ whenever $f(\mathbf{x} \cup \{v\}) > 0$, and by definition

$$\lambda(\mathbf{x}, v) = f(\mathbf{x} \cup \{v\})/f(\mathbf{x}) \quad \text{if } f(\mathbf{x}) > 0, \quad \lambda(\mathbf{x}, v) = 0 \quad \text{otherwise.}$$

This is in a one-to-one correspondence with the density f, and has the interpretation that $\lambda(\mathbf{x}, v)\rho(z)\,\mathrm{d}z\,Q(\mathrm{d}r)$ is the conditional probability of $\mathbf{X}$ having a disc with centre in an infinitesimal region containing z and of size $\mathrm{d}z$ and radius in an infinitesimal region containing r and of size $\mathrm{d}r$, given the rest of $\mathbf{X}$ is $\mathbf{x}$.

For functionals $W = A, L, \ldots$, define $W(\mathbf{x}, v) = W(\mathcal{U}_{\mathbf{x} \cup \{v\}}) - W(\mathcal{U}_{\mathbf{x}})$. The T-interaction process (6) has an hereditary density, with Papangelou conditional intensity

$$\lambda_\theta(\mathbf{x}, v) = \tag{8}$$
$$\exp\left(\theta_1 A(\mathbf{x}, v) + \theta_2 L(\mathbf{x}, v) + \theta_3 \chi(\mathbf{x}, v) + \theta_4 N_{\mathrm{h}}(\mathbf{x}, v) + \theta_5 N_{\mathrm{ic}}(\mathbf{x}, v) + \theta_6 N_{\mathrm{bv}}(\mathbf{x}, v)\right)$$

if $\mathbf{x} \cup \{v\} \in \mathcal{N}$, and $\lambda_\theta(\mathbf{x}, v) = 0$ otherwise. Note that $\mathcal{N}$ is hereditary, meaning that

$\mathbf{x} \in \mathcal{N}$ implies $\mathbf{y} \in \mathcal{N}$ if $\mathbf{y} \subset \mathbf{x}$. The process $\mathbf{X}$ is said to be *attractive* if

$$\lambda_\theta(\mathbf{x}, v) \geq \lambda_\theta(\mathbf{y}, v) \quad \text{whenever } \mathbf{y} \subset \mathbf{x},\ \mathbf{x} \in \mathcal{N} \tag{9}$$

and *repulsive* if

$$\lambda_\theta(\mathbf{x}, v) \leq \lambda_\theta(\mathbf{y}, v) \quad \text{whenever } \mathbf{y} \subset \mathbf{x},\ \mathbf{x} \in \mathcal{N}. \tag{10}$$

Note that since quarmass integrals are additive,

$$A(\mathbf{x}, v) = A(b_v) - A(b_v \cap \mathcal{U}_\mathbf{x}), \quad L(\mathbf{x}, v) = L(b_v) - L(b_v \cap \mathcal{U}_\mathbf{x}), \quad \chi(\mathbf{x}, v) = 1 - N_{\mathrm{h}}(b_v \cap \mathcal{U}_\mathbf{x}). \tag{11}$$

Proposition 2. *We have that*

(a) the A-interaction process is attractive if $\theta_1 < 0$ and repulsive if $\theta_1 > 0$;

(b) under weak conditions, e.g. if S contains an open disc, the L-interaction process is neither attractive nor repulsive if $\theta_2 \neq 0$;

(c) under other weak conditions, basically meaning that S is not too small compared to $\inf \operatorname{supp}(Q)$ (as exemplified in the proof), the W-interaction processes with $W = \chi, N_{\mathrm{h}}, N_{\mathrm{ic}}, N_{\mathrm{bv}}$ are neither attractive nor repulsive if $\theta_i \neq 0$, $i = 3, 4, 5, 6$;

(d) under similar weak conditions as in (c), the continuum random cluster model (i.e. the N_{cc}-interaction process, where $\theta_3 = \theta_4$ and $\theta_1 = \theta_2 = \theta_5 = \theta_6 = 0$) is neither attractive nor repulsive if $\theta_3 \neq 0$.

Proof. From (11) follows immediately (a), which is a well-known result [3]. We have that $L(b_v \cap \mathcal{U}_{x_1}) > 0 = L(b_v \cap \mathcal{U}_\emptyset)$ if $b_v \cap b_{x_1} \neq \emptyset$. This provides a simple example where $\lambda_{\theta_2}(\mathbf{x}, v)$ is decreasing or increasing in $\mathbf{x}$ if $\theta_2 > 0$ or $\theta_2 < 0$, respectively. On the other hand, if S contains an open disc, we may obtain the opposite case. The left panel in Figure 3 shows such an example, with four discs of equal radii, where the four centres of the discs can be made arbitrary close, and where $L(b_v \cap \mathcal{U}_{x_1,x_2,x_3}) < L(b_v \cap \mathcal{U}_{x_1,x_2})$. Thereby (b) is verified.

To verify (c)-(d) we consider again discs $b_v, b_{x_1}, b_{x_2}, \ldots$ of equal radii, since it may be possible that Q is degenerate.

Suppose that $b_v \cap b_{x_1} = \emptyset$, $b_v \cap b_{x_2} \neq \emptyset$, and $b_{x_1} \cap b_{x_2} \neq \emptyset$, and let $\mathbf{x} = \{x_1, x_2\}$. Then $\chi(\mathbf{y}, v) = 2$ and $\chi(\mathbf{x}, v) = 1$ if $\mathbf{y} = \{x_1\}$, while $\chi(\mathbf{y}, v) = 1$ and $\chi(\mathbf{x}, v) = 2$ if $\mathbf{y} = \{x_2\}$.

Since $\chi = N_{\mathrm{cc}}$ in these examples, we obtain (c) in the case of the χ-interaction process and (d) in the case of the N_{cc}-interaction process.

Suppose that b_v, b_{x_1}, b_{x_2} have no common intersection but each pair of discs are overlapping, i.e. they form a hole. If $\mathbf{y} = \{x_1, x_2\}$ and the hole disappears when we consider $\mathbf{x} = \{x_1, x_2, x_3\}$, then $N_{\mathrm{h}}(\mathbf{y}, v) = 1$ and $N_{\mathrm{h}}(\mathbf{x}, v) = 0$. Note that $N_{\mathrm{bv}}(\mathbf{y}, v) = 4$ and it may be possible that $N_{\mathrm{bv}}(\mathbf{x}, v) = 2$, as exemplified in the right panel in Figure 3. On the other hand, if $\mathbf{y} = \{x_1\}$ and $\mathbf{x} = \{x_1, x_2\}$, then $N_{\mathrm{h}}(\mathbf{y}, v) = 0$, $N_{\mathrm{h}}(\mathbf{x}, v) = 1$, $N_{\mathrm{bv}}(\mathbf{y}, v) = 2$, and $N_{\mathrm{bv}}(\mathbf{x}, v) = 4$. Hence we have established (c) in the case of the N_{h} and N_{bv}-interaction processes.

Finally, the case of the N_{ic}-interaction process in (c) follows simply by considering two overlapping discs and two disjoint discs.

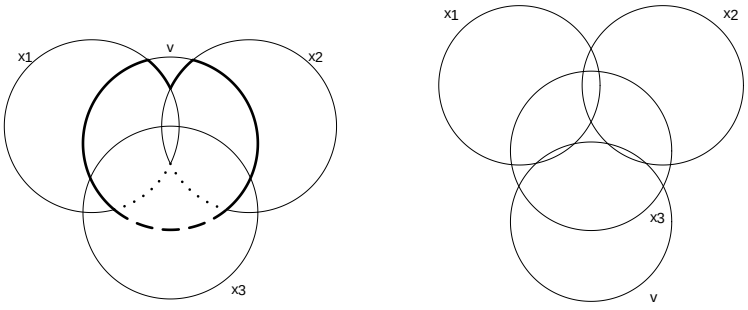

FIGURE 3: Examples of four discs of equal radii. Left panel: When we add x_3 to $\{x_1, x_2\}$ the dotted arcs disappear and the dashed arc appears, so $L(b_v \cap \mathcal{U}_{\{x_1,x_2,x_3\}}) < L(b_v \cap \mathcal{U}_{\{x_1,x_2\}})$. Right panel: $N_{\mathrm{bv}}(\{x_1, x_2\}, v) = 4$ and $N_{\mathrm{bv}}(\{x_1, x_2, x_3\}, v) = 2$.

Thus, in terms of the 'local characteristic' $\lambda_\theta(\mathbf{x}, v)$, we can easily interpret the importance of the parameter θ_1 in the A-interaction process, and also that of θ_2 in the L-interaction process provided Q is degenerate, while the role of the parameters in the other processes is less clear. Their meaning is better understood in 'global terms' and by simulation studies. Figures 4-7 show some examples of simulated realizations from a variety of models when the reference Poisson process is as specified in Figure 1. In comparison with the reference Poisson process, the A-interaction process with $\theta_1 > 0$ respective $\theta_1 < 0$ tends to produce realizations with a larger

respective smaller area $A(\mathcal{U}_{\mathbf{x}})$, and similarly for the W-interaction process, with $W = L, \chi, N_{\mathrm{h}}, N_{\mathrm{ic}}, N_{\mathrm{bv}}, N_{\mathrm{cc}}$, see Figures 4-5 and the upper left and right panels in Figure 6. However, the interpretation of (θ_1, θ_2) in the (A, L)-interaction process depends on the signs and how large these two parameters are, see the last four panels in Figure 6. Figure 7 shows examples where the minimal sufficient statistic is given by three or four geometric characteristics, whereby the meaning of the non-zero θ_i's specifying the process becomes even more complicated.

4.3. Geometric characteristics and inclusion-exclusion formulae

Lemmas 2-3 below concern various useful relations between certain geometric characteristics of the union $\mathcal{U} = \mathcal{U}_{\mathbf{x}}$ and of its power tessellation $\mathcal{B} = \mathcal{B}_{\mathbf{x}}$, assuming $\mathbf{x} \in \mathcal{N}$. Among other things, the results become useful in connection to computation of geometric characteristics in Section 4.4 and for the sequential constructions considered in Sections 3.2 and 4.7 and Appendices A-B.

Define the following characteristics of $\mathcal{B} = \mathcal{B}_{\mathbf{x}}$: the number of non-empty cells $N_{\mathrm{c}} = N_{\mathrm{c}}(\mathcal{B})$, the number of interior edges $N_{\mathrm{ie}} = N_{\mathrm{ie}}(\mathcal{B})$, the number of edges $N_{\mathrm{e}} = N_{\mathrm{be}} + N_{\mathrm{ie}}$, the number of interior vertices $N_{\mathrm{iv}} = N_{\mathrm{iv}}(\mathcal{B})$, and the number of vertices $N_{\mathrm{v}} = N_{\mathrm{bv}} + N_{\mathrm{iv}}$. These statistics do not appear in the specification (4) since they cannot be determined from $\mathcal{U}$ but only from $\mathcal{B}$. Furthermore, let $N = n(\mathbf{x})$ denote the number of discs.

Lemma 2. *We have*

$$N_{\mathrm{ic}} \leq N_{\mathrm{cc}} \leq N_{\mathrm{c}} \leq N, \quad N_{\mathrm{bv}} = 2N_{\mathrm{ie}} - 3N_{\mathrm{iv}} \tag{12}$$

and

$$\chi = N_{\mathrm{cc}} - N_{\mathrm{h}} = N_{\mathrm{c}} - N_{\mathrm{ie}} + N_{\mathrm{iv}}. \tag{13}$$

If $N_{\mathrm{c}} \geq 2$ *and* $N_{\mathrm{cc}} = 1$*, then*

$$N_{\mathrm{be}} = N_{\mathrm{bv}} \leq 2N_{\mathrm{ie}}, \quad 3N_{\mathrm{v}} = 2N_{\mathrm{e}}. \tag{14}$$

If $N_{\mathrm{c}} \geq 3$ *and* $N_{\mathrm{cc}} = 1$*, then*

$$N_{\mathrm{ie}} \leq 3N_{\mathrm{c}} - 6. \tag{15}$$

Moreover,

$$N_{\mathrm{bv}} \leq 6N \tag{16}$$

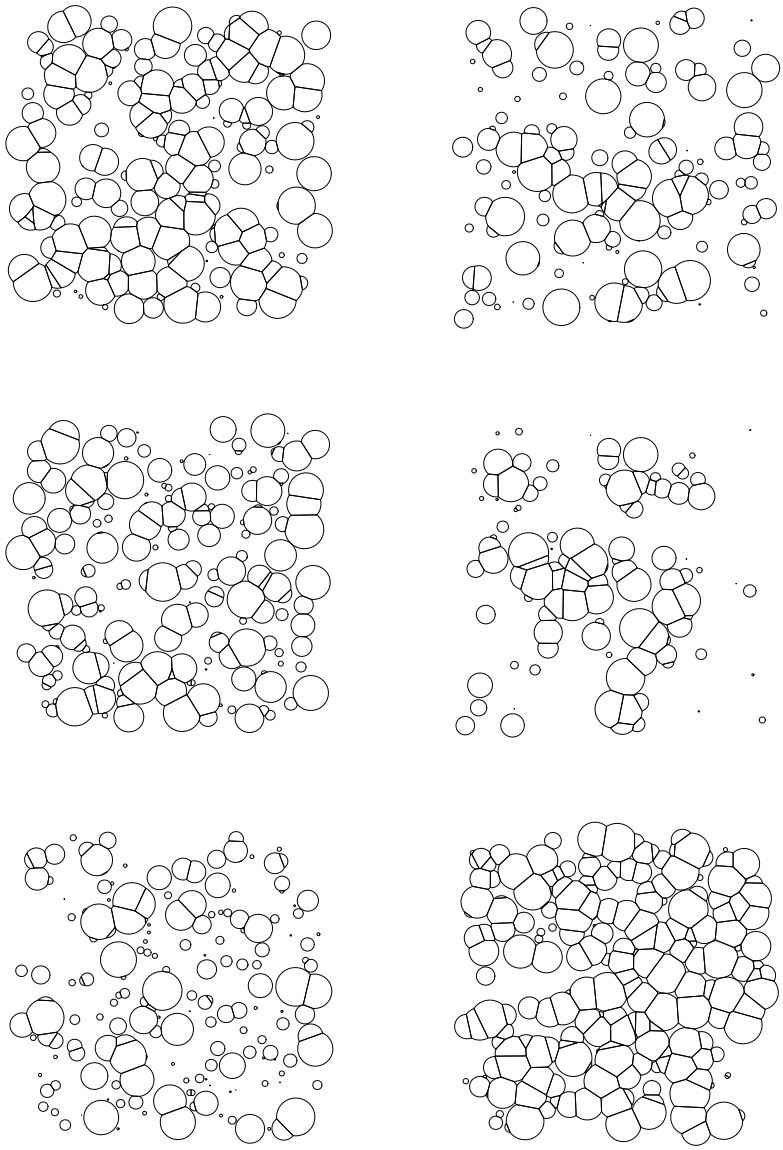

FIGURE 4: Simulated realizations of the A-interaction process with $\theta_1 = 0.1$ (upper left panel) and $\theta_1 - 0.1$ (upper right panel), the L-interaction process with $\theta_2 = 0.2$ (middle left panel) and $\theta_2 = -0.2$ (middle right panel), and the χ-interaction process with $\theta_3 = 1$ (lower left panel) and $\theta_3 = -1$ (lower right panel).

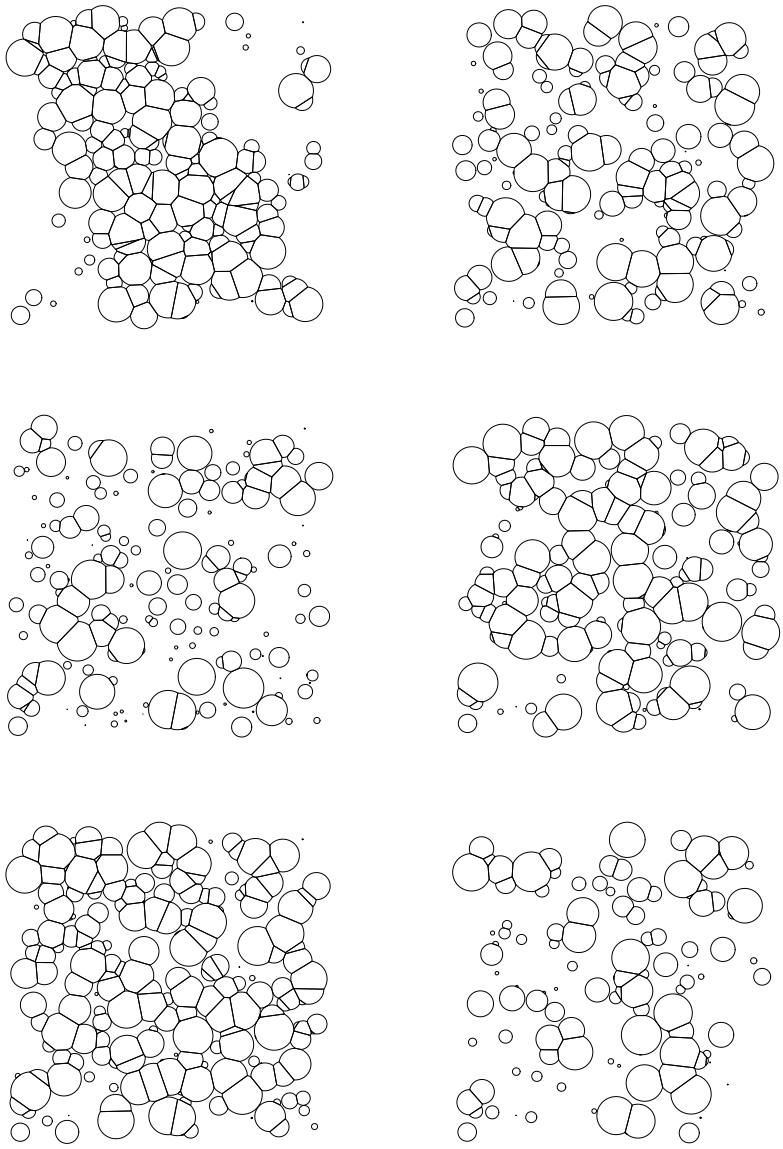

FIGURE 5: Simulated realizations of the N_{h}-interaction process with $\theta_4 = 3$ (upper left panel) and $\theta_4 = -3$ (upper right panel), the N_{ic}-interaction process with $\theta_5 = 0.7$ (middle left panel) and $\theta_5 = -1$ (middle right panel), and the N_{bv}-interaction process with $\theta_6 = 0.2$ (lower left panel) and $\theta_6 = -0.2$ (lower right panel).

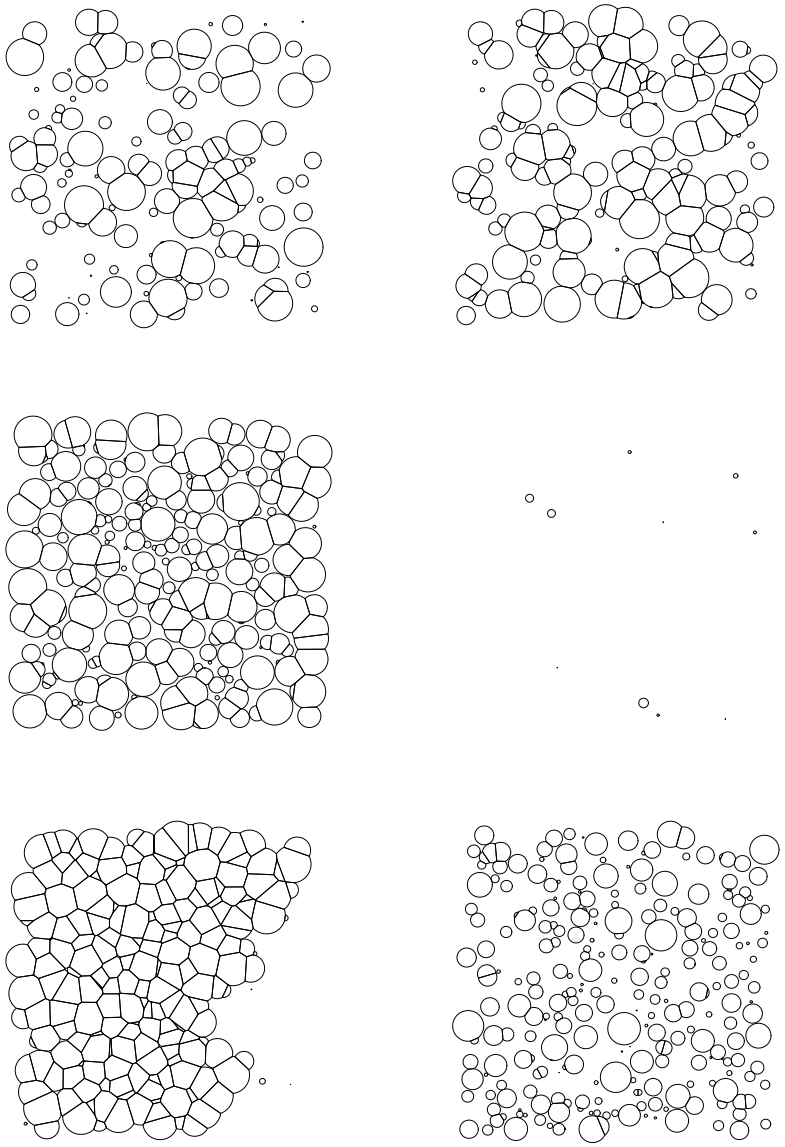

FIGURE 6: Simulated realizations of the N_{cc}-interaction process with $\theta_3 = \theta_4 = 0.5$ (upper left panel) and $\theta_3 = \theta_4 = -0.5$ (upper right panel), and the (A, L)-interaction process with $(\theta_1, \theta_2) = (1, 1)$ (middle left panel), $(\theta_1, \theta_2) = (-1, -1)$ (middle right panel), $(\theta_1, \theta_2) = (0.6, -1)$ (lower left panel), and $(\theta_1, \theta_2) = (-1, 1)$ (lower right panel).

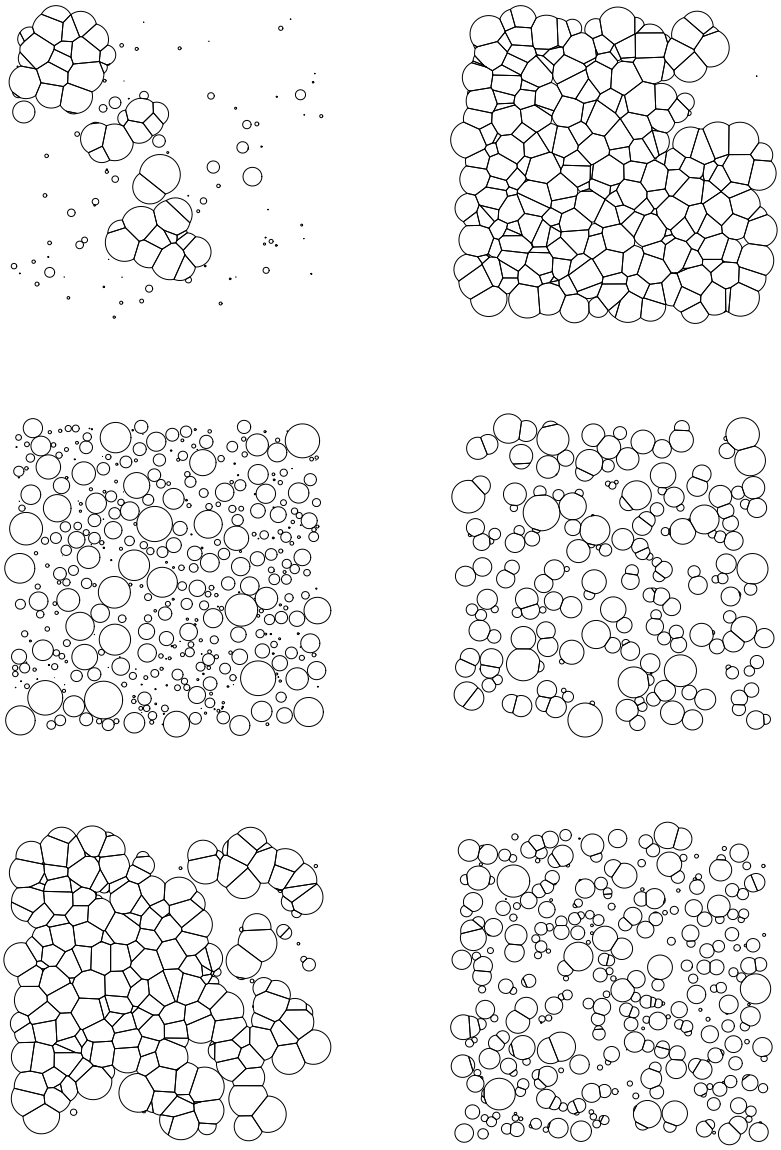

FIGURE 7: Simulated realizations of the (A, L, N_{cc})-interaction process with $(\theta_1, \theta_2) = (0.6, -1)$ and $\theta_3 = \theta_4 = 2$ (upper left panel) or $\theta_3 = \theta_4 = -1$ (upper right panel), the (A, L, N_{ic})-interaction process with $(\theta_1, \theta_2) = (-1, 1)$ and $\theta_5 = 5$ (middle left panel) or $\theta_5 = -5$ (middle right panel), and the $(A, L, \chi, N_{\mathrm{ic}})$-interaction process with $(\theta_3, \theta_5) = (2, -2)$ and $(\theta_1, \theta_2) = (0.6, -1)$ (lower left panel) or $(\theta_1, \theta_2) = (-1, 1)$ (lower right panel).

and

$$N_{\mathrm{h}} = 0 \quad \textit{if } N_{\mathrm{c}} \leq 2, \qquad N_{\mathrm{h}} \leq 2N_{\mathrm{c}} - 5 \quad \textit{if } N_{\mathrm{c}} \geq 3. \tag{17}$$

Proof. The inequalities in (12) clearly hold, and the identity in (12) follows from a simple counting argument, using that each interior edge has two endpoints, and exactly three interior edges emerge at each interior vertex.

The first identity in (13) is just the definition (3), and the second identity follows from Euler's formula.

Assuming $N_{\mathrm{c}} \geq 2$ and $N_{\mathrm{cc}} = 1$, (14) follows from simple counting arguments, using first that exactly two boundary edges emerge at each boundary vertex, second the simple fact that $N_{\mathrm{bv}} \leq N_{\mathrm{v}}$, and third that exactly three edges emerge at each vertex.

To verify (15), consider the dual graph $\mathcal{D}$. Since we assume that $N_{\mathrm{c}} \geq 3$ and $N_{\mathrm{cc}} = 1$, $\mathcal{D}$ has N_{ie} edges and N_{c} vertices, and so by planar graph theory [44], since $\mathcal{D}$ is a connected graph without multiple edges, the number of dual edges is bounded by $3N_{\mathrm{c}} - 6$.

To verify (16), note that $N_{\mathrm{bv}} \leq 2N_{\mathrm{ie}}$, cf. (12). Using (15) and considering a sum over all components, we obtain that N_{ie} is bounded above by the number of components with two cells plus three times the number of components with three or more cells. Consequently, $N_{\mathrm{bv}} \leq 6N$.

Finally, to verify (17), note that N_{h} is given by the sum of number of holes of all connected components of $\mathcal{U}$, and a connected component consisting of one or two power cells has no holes, so it suffices to consider the case where $N_{\mathrm{cc}} = 1$ and $N_{\mathrm{c}} \geq 3$. Then by (13), N_{h} is bounded above by $1 - (N_{\mathrm{c}} - N_{\mathrm{ie}})$, which in turn by (15) is bounded above by $2N_{\mathrm{c}} - 5$.

Equation (17) is a main result in [19]. Our proof of (17) is much simpler and shorter, demonstrating the usefulness of the power tessellation and its dual graph. The upper bound in (17) can be obtained for any three or more discs: If $\mathbf{x}$ consists of three discs b_1, b_2, b_3 such that $b_i \cap b_j \neq \emptyset$ for $1 \leq i < j \leq 3$ and $b_1 \cap b_2 \cap b_3 = \emptyset$, then $N_{\mathrm{h}} = 1$ and $N_{\mathrm{c}} = 3$, so $N_{\mathrm{h}} = 2N_{\mathrm{c}} - 5$. Furthermore, we may add a fourth, fifth, ... disc, where each added disc generates two new holes—as illustrated in Figure 8 in the case of five discs—whereby $N_{\mathrm{c}} = 3, 4, \ldots$ and $N_{\mathrm{h}} = 2N_{\mathrm{c}} - 5$ in each case.

Kendall, van Lieshout and Baddeley [19] noticed the inclusion-exclusion formula for

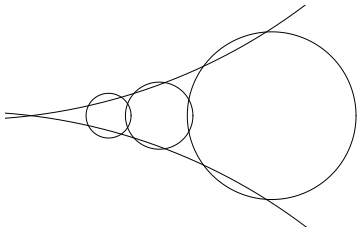

FIGURE 8: A configurations of five discs with exactly $2N_c - 5$ holes.

the functionals $W = A, L, \chi$:

$$W(\mathcal{U}_{\mathbf{x}}) = \sum_{1}^{n} W(b_i) - \sum_{1 \le i < j \le n} W(b_i \cap b_j) + \cdots + (-1)^{n-1} W(b_1 \cap \cdots \cap b_n) \qquad (18)$$

where the sums involve $2^n - 1$ terms. Using the power tessellation, inclusion-exclusion formulae with much fewer terms are given by (12)-(13) for χ and N_{bv}, and by Lemma 3 below for A and L. In Lemma 3, $I_1(\mathbf{x})$, $I_2(\mathbf{x})$, and $I_3(\mathbf{x})$ denote index sets corresponding to non-empty cells, interior edges, and interior vertices of $\mathcal{B}_{\mathbf{x}}$, respectively. For later use in Section 4.5, note that $I_1(\mathbf{x})$ and $I_2(\mathbf{x})$ correspond to the cliques in the dual graph $\mathcal{D}_{\mathbf{x}}$ consisting of 1 and 2 nodes, respectively, while $I_3(\mathbf{x})$ corresponds to the subset of 3-cliques $\{i, j, k\} \in \mathcal{D}_{\mathbf{x}}$ with $b_i \cap b_j \cap b_k \neq \emptyset$ (i.e. $b_i \cup b_j \cup b_k$ has no hole). Note that if $\{i, j, k\} \in \mathcal{D}_{\mathbf{x}}$, then $b_i \cap b_j \cap b_k \neq \emptyset$ if and only if $E_{i,j} \cap E_{i,k} \neq \emptyset$, where the latter property is easily checked.

Lemma 3. *The following inclusion-exclusion formulae hold for the area and perimeter of the union of discs:*

$$A(\mathcal{U}_{\mathbf{x}}) = \sum_{i \in I_1(\mathbf{x})} A(b_i) - \sum_{\{i,j\} \in I_2(\mathbf{x})} A(b_i \cap b_j) + \sum_{\{i,j,k\} \in I_3(\mathbf{x})} A(b_i \cap b_j \cap b_k) \qquad (19)$$

$$= \sum_{i \in I_1(\mathbf{x})} A(B_i) \qquad (20)$$

and

$$L(\mathcal{U}_{\mathbf{x}}) = \sum_{i \in I_1(\mathbf{x})} L(b_i) - \sum_{\{i,j\} \in I_2(\mathbf{x})} L(b_i \cap b_j) + \sum_{\{i,j,k\} \in I_3(\mathbf{x})} L(b_i \cap b_j \cap b_k) \qquad (21)$$

$$= \sum_{e \text{ boundary edge of } \mathcal{B}_{\mathbf{x}}} L(e). \qquad (22)$$

Proof. Equations (19) and (21) are due to Theorem 6.2 in [10], while (20) and (22) follow immediately.

Edelsbrunner [10] establishes extensions to $\mathbb{R}^d$ of the inclusion-exclusion formulae given by the second identities in (12), (19), and (21). Note that we cannot replace the sums in (19) by sums over all discs, pairs of discs, and triplets of discs from $\mathbf{x}$.

4.4. Local calculations

For calculating the area and perimeter, the inclusion-exclusion formulae (20) and (22) appear to be more suited than (19) and (21) when the computations are done in combination with the sequential constructions considered in Sections 3.2 and 4.7 and Appendices A-B. Note that we need only to do "local computations".

For example, suppose we are given the power tessellation $\mathcal{B}^{\mathrm{old}}$ of $\mathcal{U}^{\mathrm{old}} = \cup_1^{n-1} b_i$ and add a new disc b_n. When constructing the new power tessellation $\mathcal{B}^{\mathrm{new}}$ of $\mathcal{U}^{\mathrm{new}} = \cup_1^{n} b_i$, we need only to consider the new set B_n and the old cells in $\mathcal{B}^{\mathrm{old}}$ which are neighbours to B_n with respect to the dual graph of $\mathcal{B}^{\mathrm{new}}$ (see Appendix A). Similarly, when a disc is deleted and the new tessellation is constructed, we need only local computations with respect to the discs intersecting the disc which is deleted (see Appendix B); we study this neighbour relation given by overlapping discs in Section 4.5. Moreover, local computations are only needed when calculating N_{ic} and N_{bv}.

In order to calculate (χ, N_{h}) or equivalently $(N_{\mathrm{cc}}, N_{\mathrm{h}})$, we could keep track on the inner and outer boundary curves in our sequential constructions, using a clockwise and anti-clockwise orientation for the two different types of boundary curves. However, in our MCMC simulation codes, we found it easier to keep track on $N_{\mathrm{c}}, N_{\mathrm{ie}}, N_{\mathrm{iv}}$, and N_{cc}, and thereby obtain χ by the second equality in (13), and hence N_{h} by the first inequality in (13). In either case, this is another kind of local computation, where the relevant neighbour relation is the connected component relation studied in Section 4.5.

Finally, let us explain in more detail how we can find the area A. We can easily determine the total area of all isolated cells of $\mathcal{B}$. Suppose that B_i is a non-empty, non-isolated cell of $\mathcal{B}$. Let c_i denote the arithmetic average of the vertices of B_i. Then $c_i \in B_i$, since B_i is convex. For any three points $c, u, v \in \mathbb{R}^2$, let $\Delta(c, u, v)$ denote the triangle with vertices c, u, v. If $\lfloor u, v \rceil$ is a boundary edge of B_i, let $\Gamma(u, v)$ denote the cap of b_i bounded by the arc $\lfloor u, v \rceil$ and the line segment $[u, v]$. Then the area of B_i is the sum of areas of all triangles $\Delta(c_i, u, v)$, where u and v are defining an (interior or boundary) edge of B_i, plus the sum of areas of all caps $\Gamma(u, v)$, where u and v are

defining a boundary edge of B_i.

4.5. Markov properties

The various Markov point process models considered in this section are either specified by a local Markov property in terms of the Papangelou conditional intensity or by a particular form of the density given by a Hammersley-Clifford type theorem [2, 37]. Particularly, we show that it is useful to view the T-interaction process (6) as a connected component Markov point process, where we show how a spatial Markov property becomes useful for handling edge effects. Throughout Sections 4.5.1-4.5.5, we let $\mathbf{x} \in \mathcal{N}$.

4.5.1. *Local Markov property in terms of the overlap relation:* Consider the overlap relation $\sim$ defined on $S \times (0, \infty)$ by $u \sim v$ if and only if $b(u) \cap b(v) \neq \emptyset$. The T-interaction process is said to be Markov with respect to $\sim$ if $\lambda_\theta(\mathbf{x}, v)$ depends only on $\mathbf{x}$ through $\{u \in \mathbf{x} : u \sim v\}$, i.e. the neighbours in $\mathbf{x}$ to v. Kendall, van Lieshout and Baddeley [19] observed that the quarmass-interaction process is Markov with respect to $\sim$. The following proposition generalizes this result.

Proposition 3. *The T-interaction process with density (6) is Markov with respect to the overlap relation if and only if $\theta_4 = \theta_5 = 0$.*

Proof. In other words, with respect to the overlap relation $\sim$, we have to verify that the A, L, χ, and N_{bv}-interaction processes are Markov, while the N_{h} and N_{ic}-interaction processes are not Markov. It follows immediately from (8) and (11) that the A, L, and χ-interaction processes are Markov, and Figures 9-10 show that the N_{h} and N_{ic}-interaction processes are not Markov. If w is a boundary vertex of $\mathcal{U}_{\mathbf{x}}$ but not of $\mathcal{U}_{\mathbf{x}\cup\{v\}}$, then w is contained in the disc v. If instead w is a boundary vertex of $\mathcal{U}_{\mathbf{x}\cup\{v\}}$ but not of $\mathcal{U}_{\mathbf{x}}$, then w is given by the intersection of the boundaries of v and an $\mathbf{x}$-disc. Consequently, $N_{\mathrm{bv}}(\mathbf{x}, v) = N_{\mathrm{bv}}(\mathcal{U}_{\mathbf{x}\cup\{v\}}) - N_{\mathrm{bv}}(\mathcal{U}_{\mathbf{x}})$ depends on $\mathbf{x}$ only through $\{u \in \mathbf{x} : u \sim v\}$, so the N_{bv}-interaction process is Markov. This completes the proof.

As noticed in [19], using the inclusion-exclusion formula (18), the Hammersley-Clifford representation [37] of the quarmass-interaction process is

$$f_{(\theta_1,\theta_2,\theta_3)}(\mathbf{x}) = \prod_{\mathbf{y}\subseteq\mathbf{x}} \phi_{(\theta_1,\theta_2,\theta_3)}(\mathbf{y}) \tag{23}$$

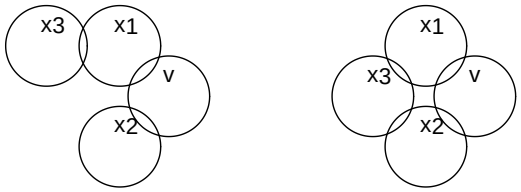

FIGURE 9: An example showing that N_{h}-interaction process is not Markov with respect to the overlap relation: both $N_{\mathrm{h}}(\mathbf{x}, v) = 0$ (left panel) and $N_{\mathrm{h}}(\mathbf{x}, v) = 1$ (right panel) depend on the disc x_3 which is not overlapping the disc v.

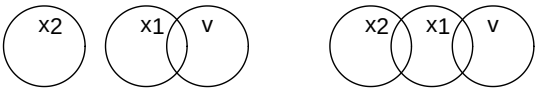

FIGURE 10: An example showing that N_{ic}-interaction process is not Markov with respect to the overlap relation: both $N_{\mathrm{ic}}(\mathbf{x}, v) = -1$ (left panel) and $N_{\mathrm{ic}}(\mathbf{x}, v) = 0$ (right panel) depend on the disc x_2 which is not overlapping the disc v.

where the interaction function is given by

$$\phi_{(\theta_1,\theta_2,\theta_3)}(\mathbf{x}) = \exp\left((-1)^n \left(\theta_1 A(\cap_1^n b_i) + \theta_2 L(\cap_1^n b_i) + \theta_3 \chi(\cap_1^n b_i)\right)\right) \tag{24}$$

for non-empty $\mathbf{x} = \{(z_1, r_1), \ldots, (z_n, r_n)\}$, and $\phi_{(\theta_1,\theta_2,\theta_3)}(\emptyset) = 1/c_{(\theta_1,\theta_2,\theta_3)}$. However, for at least two reasons, it is the density in (6) of the quarmass-interaction process rather than the Hammersley-Clifford representation (23) which seems appealing. First, the process has interactions of all orders, since $\log \phi_{(\theta_1,\theta_2,\theta_3)}(\mathbf{x})$ can be non-zero no matter how many discs $\mathbf{x}$ specifies, so the calculation of the interaction function (24) can be very time consuming. Second, (23) seems not to be of much relevance if we cannot observe $\mathbf{X}$ but only $\mathcal{U}_{\mathbf{X}}$. This indicates that another kind of neighbour relation is needed when describing the Markov properties. Two other relations are therefore discussed below.

4.5.2. *Local Markov property in terms of the dual graph:* Applying the inclusion-exclusion formulae given by the last identity in (13), (19), and (21), we obtain another representation of the quarmass-interaction process density, namely as a product of terms corresponding to the cliques in the dual graph, excluding the case of 3-cliques

$\{i,j,k\} \in \mathcal{D}_{\mathbf{x}}$ with $b_i \cap b_j \cap b_k = \emptyset$:

$$f_{(\theta_1,\theta_2,\theta_3)}(\mathbf{x}) = \frac{1}{c_{(\theta_1,\theta_2,\theta_3)}} \times \prod_{i \in I_1(\mathbf{x})} \phi_{(\theta_1,\theta_2,\theta_3)}(x_i) \times \prod_{\{i,j\} \in I_2(\mathbf{x})} \phi_{(\theta_1,\theta_2,\theta_3)}(\{x_i,x_j\}) \quad (25)$$
$$\times \prod_{\{i,j,k\} \in I_3(\mathbf{x})} \phi_{(\theta_1,\theta_2,\theta_3)}(\{x_i,x_j,x_k\})$$

where now

$$\phi_{(\theta_1,\theta_2,\theta_3)}(x_i) = \exp\left(\theta_1 A(b_i) + \theta_2 L(b_i) + \theta_3\right),$$
$$\phi_{(\theta_1,\theta_2,\theta_3)}(\{x_i,x_j\}) = \exp\left(-\theta_1 A(b_i \cap b_j) - \theta_2 L(b_i \cap b_j) - \theta_3\right),$$
$$\phi_{(\theta_1,\theta_2,\theta_3)}(\{x_i,x_j,x_k\}) = \exp\left(\theta_1 A(b_i \cap b_j \cap b_k) + \theta_2 L(b_i \cap b_j \cap b_k) + \theta_3\right).$$

This is of a somewhat similar form as the Hammersley-Clifford representation for a nearest-neighbour Markov point process [2] with respect to the neighbour relation defined by the dual graph (it is not exactly of the required form, since in (25) we do not have a product over all $u \in \mathbf{x}$ but only over those u generating non-empty cells in $\mathcal{B}_{\mathbf{x}}$). In fact, since it can be verified that the relation satisfies certain consistency conditions (Theorem 4.13 in [2]), the quarmass-interaction process is not exactly a nearest-neighbour Markov point process with respect to the dual graph (but it is a nearest-neighbour Markov point process if instead we consider a relation similar to the iterated Dirichlet relation in [2]). On the other hand, the identity in (12) implies that

$$f_{\theta_6}(\mathbf{x}) = \frac{1}{c_{\theta_6}} \times \prod_{\{i,j\} \in I_2(\mathbf{x})} \exp(2\theta_6) \times \prod_{\{i,j,k\} \in I_3(\mathbf{x})} \exp(-3\theta_6) \quad (26)$$

which shows that the N_{bv}-interaction process is a nearest-neighbour Markov point process with respect to the dual graph. Moreover, for the N_{h} and N_{ic}-interaction processes, it seems not possible to obtain a kind of Hammersley-Clifford representation with respect to the dual graph. Note that (25) and (26) seem not to be of much relevance if we cannot observe $\mathbf{X}$ but only $\mathcal{U}_{\mathbf{X}}$.

4.5.3. *Local Markov property in terms of the connected components:* In our opinion, the most relevant results are Propositions 4-5 below, where the first proposition states that $\mathbf{X}$ is a connected component Markov point process [2, 4, 7, 30], and the second proposition specifies a spatial Markov property. As explained in further detail in [2], for a connected component Markov point process, the Papangelou conditional intensity

depends only on local information with respect to the connected component relation $\sim_{\mathbf{x}}$ defined as follows: for $u, v \in \mathbf{x}$, $u \sim_{\mathbf{x}} v$ if and only if $b(u)$ and $b(v)$ are contained in the same connected component K of $\mathcal{U}_{\mathbf{x}}$. Thereby MCMC computations become "local", as discussed further in Section 4.7. The spatial Markov property is discussed in Sections 4.5.4-4.5.5.

Proposition 4. *The T-interaction process with density (6) is a connected component Markov point process.*

Proof. The density is of the form

$$\frac{1}{c_\theta} \prod_{K \in \mathcal{K}(\mathcal{U}_{\mathbf{x}})} \exp\left(\theta_1 A(K) + \theta_2 L(K) + \theta_3 \chi(K) + \theta_4 N_{\mathrm{h}}(K) + \theta_5 N_{\mathrm{ic}}(K) + \theta_6 N_{\mathrm{bv}}(K)\right) \tag{27}$$

where $\mathcal{K}(\mathcal{U}_{\mathbf{x}})$ is the set of connected components of $\mathcal{U}_{\mathbf{x}}$. Thus, by Lemma 1 in [4]), it is a connected component Markov point process.

In the discrete case (discs replaced by pixels), a Markov connected component field [32], which is also assumed to be a second order Markov random field, has a density of a similar form as (27).

4.5.4. *Spatial Markov property in terms of the overlap relation:* Consider again the quarmass-interaction process, and for the moment assume that $R = \mathrm{supp}(Q) < \infty$. Let $W_{\ominus 2R} = \{u \in W : b(u, 2R) \subseteq W\}$ be the $2R$-clipped window of points in W so that almost surely no disc of $\mathbf{X}$ with centre in $W_{\ominus 2R}$ intersect another disc of $\mathbf{X}$ with centre in $W^c = S \setminus W$. Split $\mathbf{X}$ into $\mathbf{X}^{(1)}$, $\mathbf{X}^{(2)}$, $\mathbf{X}^{(3)}$ corresponding to discs with centres in $W_{\ominus 2R}$, $W \setminus W_{\ominus 2R}$, W^c, respectively. The spatial Markov property [37] states that $\mathbf{X}^{(1)}$ and $\mathbf{X}^{(3)}$ are conditionally independent given $\mathbf{X}^{(2)}$, and the conditional distribution $\mathbf{X}^{(1)}|\mathbf{X}^{(2)} = \mathbf{x}^{(2)}$ has density

$$f_{\theta_1,\theta_2,\theta_3}(\mathbf{x}^{(1)}|\mathbf{x}^{(2)}) = \tag{28}$$
$$\frac{1}{c_{\theta_1,\theta_2,\theta_3}(\mathbf{x}^{(2)})} \exp\left(\theta_1 A(\mathcal{U}_{\mathbf{x}^{(1)} \cup \mathbf{x}^{(2)}}) + \theta_2 L(\mathcal{U}_{\mathbf{x}^{(1)} \cup \mathbf{x}^{(2)}}) + \theta_3 \chi(\mathcal{U}_{\mathbf{x}^{(1)} \cup \mathbf{x}^{(2)}})\right)$$

with respect to the reference Poisson process $\mathbf{\Psi}$ restricted to discs with centres in the $2R$-clipped window. This is also a Markov point process with respect to the overlap

relation restricted to $W_{\ominus 2R}$, since the Papangelou conditional intensity $\lambda_\theta(\mathbf{x}^{(1)}, v|\mathbf{x}^{(2)})$ corresponding to (28) is related to that in (8) by

$$\lambda_\theta(\mathbf{x}^{(1)}, v|\mathbf{x}^{(2)}) = \lambda_\theta(\mathbf{x}^{(1)} \cup \mathbf{x}^{(2)}, v). \tag{29}$$

However, it is problematic to use this conditional process in practice, since both (28) and (29) depend on $\mathcal{U}_{\mathbf{x}^{(2)}} \setminus W$ which is not observable.

4.5.5. *Spatial Markov property in terms of the connected component relation:* The following spatial Markov property is more useful and applies for the general case of the T-interaction process (6) using that it is a connected component Markov point process (see also [20, 30]). We split $\mathbf{X}$ into $\mathbf{X}^{(a)}$, $\mathbf{X}^{(b)}$, $\mathbf{X}^{(c)}$ corresponding to discs belonging to connected components of $\mathcal{U}_{\mathbf{X}}$ which are respectively (a) contained in W, (b) intersecting both W and W^c, (c) contained in W^c, see Figure 11. Furthermore, let $\mathbf{x}^{(b)}$ denote any feasible realization of $\mathbf{X}^{(b)}$, i.e. $\mathbf{x}^{(b)}$ is a finite configuration of discs such that K intersects both W and W^c for all $K \in \mathcal{K}(\mathcal{U}_{\mathbf{x}^{(b)}})$.

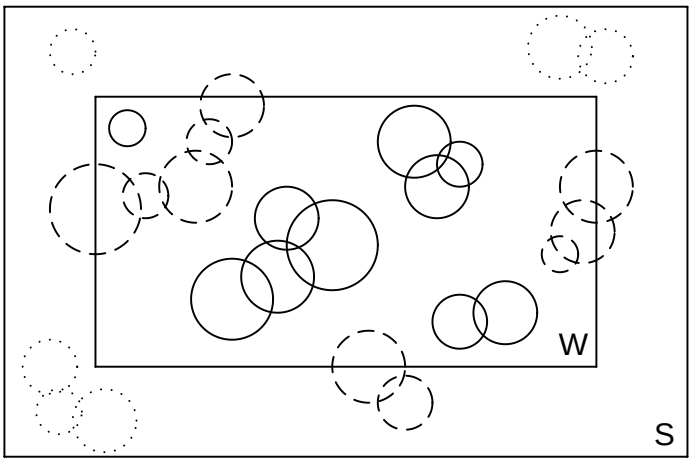

FIGURE 11: Illustrating possible realizations of $\mathbf{X}^{(a)}$ (the full circles), $\mathbf{X}^{(b)}$ (the dashed circles), and $\mathbf{X}^{(c)}$ (the dotted circles).

Proposition 5. *Conditional on $\mathbf{X}^{(b)} = \mathbf{x}^{(b)}$, we have that $\mathbf{X}^{(a)}$ and $\mathbf{X}^{(c)}$ are independent, and the conditional distribution of $\mathbf{X}^{(a)}$ depends only on $\mathbf{x}^{(b)}$ through $V =$*

$W \cap \mathcal{U}_{\mathbf{x}^{(b)}}$ and has density

$$f_\theta(\mathbf{x}^{(a)}|V) = \frac{1}{c_\theta(V)} \mathbf{1}[\mathcal{U}_{\mathbf{x}^{(a)}} \subseteq W \setminus V] \exp\Big(\theta \cdot T(\mathbf{x}^{(a)})\Big) \tag{30}$$

with respect to the reference Poisson process of discs.

Proof. Let Π denote the distribution of $\mathbf{\Psi}$ restricted to those finite configurations of discs with centres in S, and let h_θ denote the unnormalized density given by the exponential term in (27). Recall the 'Poisson expansion' (see e.g. [33])

$$\begin{aligned}
\mathrm{P}(\mathbf{X} \in F) =& \frac{1}{c_\theta} \int_F h_\theta(\mathbf{x}) \, \Pi(\mathrm{d}\mathbf{x}) \\
=& \frac{1}{c_\theta} \exp\left(- \int_S \rho(u) \, \mathrm{d}u \right) \times \\
& \sum_{n=0}^{\infty} \frac{1}{n!} \int_S \int \cdots \int_S \int h_\theta(\mathbf{x}) \mathbf{1}[\mathbf{x} \in F] \rho(u_1) \, \mathrm{d}u_1 Q(\mathrm{d}r_1) \cdots \rho(u_n) \, \mathrm{d}u_n Q(\mathrm{d}r_n)
\end{aligned}$$

(where the term with $n = 0$ is read as one if the empty configuration is in the event F and zero otherwise). From this and (27) we obtain that $(\mathbf{X}^{(a)}, \mathbf{X}^{(b)}, \mathbf{X}^{(c)})$ has joint density

$$\begin{aligned}
f(\mathbf{x}^{(a)}, \mathbf{x}^{(b)}, \mathbf{x}^{(c)}) =& \frac{1}{c_\theta} \mathbf{1}[\mathcal{U}_{\mathbf{x}^{(a)}} \subseteq W \setminus \mathcal{U}_{\mathbf{x}^{(b)}}] h_\theta(\mathbf{x}^{(a)}) \mathbf{1}[\mathcal{U}_{\mathbf{x}^{(c)}} \subseteq W^c \setminus \mathcal{U}_{\mathbf{x}^{(b)}}] h_\theta(\mathbf{x}^{(c)}) \\
& \times \mathbf{1}[\forall K \in \mathcal{K}(\mathcal{U}_{\mathbf{x}^{(b)}}) : \, K \cap W \neq \emptyset, \, K \cap W^c \neq \emptyset] h_\theta(\mathbf{x}^{(b)})
\end{aligned}$$

with respect to the product measure $\exp\big(2 \int_S \rho(u) \, \mathrm{d}u\big) \, \Pi \times \Pi \times \Pi$. Thereby the proposition follows.

The density (30) may be useful for statistical applications, since it accounts for edge effects and depends only on the union of discs intersected by the observation window W. It is a hereditary density of a connected component Markov point process with discs contained in $W \setminus V$. Its Papangelou conditional intensity $\lambda_\theta(\mathbf{x}^{(a)}, v|V)$ is simply given by

$$\lambda_\theta(\mathbf{x}^{(a)}, v|V) = \lambda_\theta(\mathbf{x}^{(a)}, v) \mathbf{1}[\mathcal{U}_{\mathbf{x}^{(a)} \cup \{v\}} \subseteq W \setminus V]. \tag{31}$$

4.6. Stability

Consider the 'unnormalized density' $h_\theta(\mathbf{x}) = \exp(\theta \cdot T(\mathbf{x}))$ corresponding to the T-interaction process with density f_θ given in (6), and recall the definition (5) of the parameter space Θ. In fact, we have yet not verified that $c_\theta \equiv \mathrm{E} h_\theta(\mathbf{\Psi} \cap (S \times (0, \infty))$ is

finite for $\theta \in \Theta$, and hence that $f_\theta = h_\theta/c_\theta$ is a well-defined density with respect to the reference Poisson process $\mathbf{\Psi}$ if $\theta \in \Theta$. This section discusses two stability properties which imply integrability of h_θ as well as other desirable properties.

4.6.1. *Ruelle stability:* This means that there exist positive constants α and β such that $h_\theta(\mathbf{x}) \le \alpha\beta^{n(\mathbf{x})}$ for all $\mathbf{x} \in \mathcal{N}$ (in fact, this and other stability properties mentioned in this paper need only to hold almost surely with respect to $\mathbf{\Psi}$, however, for ease of presentation we shall ignore such nullsets). Ruelle stability implies that $c_\theta \le \alpha \exp\big((\beta-1)\int_S \rho(z)\,\mathrm{d}z\big) < \infty$, and we say that $f_\theta = h_\theta/c_\theta$ is a *Ruelle stable density*. Other implications of Ruelle stability are discussed in Section 2.1 of [19] and the references therein.

The main question addressed in [19] is to establish Ruelle stability of the quarmass-interaction process, and the following proposition provides a very easy proof of this issue in connection to the general case of the T-interaction process (6) (since the proof is based on Lemma 2, the usefulness of the power tessellation is once again demonstrated).

Proposition 6. *For all $\theta \in \Theta$, $c_\theta < \infty$ and f_θ in (6) is a Ruelle stable density. If $\theta \in \mathbb{R}^6 \setminus \Theta$, then $c_\theta = \infty$.*

Proof. Note that a finite product of Ruelle stable functions is a Ruelle stable function. Let θ_0 denote a real parameter. From Lemma 2 follows that χ, N_{h}, N_{ic}, and N_{bv} are bounded above by $6N$, so the functions $\exp(\theta_0 W)$, $W = \chi, N_{\mathrm{h}}, N_{\mathrm{ic}}, N_{\mathrm{bv}}$ are Ruelle stable for all $\theta_0 \in \mathbb{R}$. Moreover, $\exp(\theta_1 A + \theta_2 L)$ is Ruelle stable if $a \equiv \int \exp\big(\pi\theta_1 r^2 + 2\pi\theta_2 r\big)\, Q(\mathrm{d}r)$ is finite, since $\exp(\theta_1 A + \theta_2 L) \le \exp\big((a-1)\int_S \rho(z)\,\mathrm{d}z\big)$. On the other hand, the first term in the infinite sum in (2) is a times $\exp(\theta_3 + \theta_5)\int_S \rho(z)\,\mathrm{d}z$, where $\int_S \rho(z)\,\mathrm{d}z > 0$, cf. Section 2.1. Consequently, $c_\theta = \infty$ if $a = \infty$.

4.6.2. *Local stability:* This means that there exists a constant β such that for all $\mathbf{x} \in \mathcal{N}$ and all $v \in \Omega \setminus \mathbf{x}$,

$$\lambda_\theta(\mathbf{x}, v) \le \beta. \tag{32}$$

This property is clearly implying Ruelle stability. Local stability is useful when establishing geometric ergodicity of MCMC algorithms ([13, 33]; see also Section 4.7), and it is needed in order to apply the dominating coupling from the past algorithm in [18, 22] for making perfect simulations. Note that a finite product of locally stable

functions is a locally stable function, since its Papangelou conditional intensity is given by a product of uniformly bounded Papangelou conditional intensities. The Papangelou conditional intensity (6) is a product of Papangelou conditional intensities corresponding to functions $h_{\theta_0}(\mathbf{x}) = \exp(\theta_0 W(\mathcal{U}_{\mathbf{x}}))$, with $W = A, L, \ldots$ and $\theta_0 = \theta_1, \theta_2, \ldots$.

As shown below, the picture of whether local stability is satisfied or not depends much on the particular type of model. When we in the following proposition write 'in general', the proof of the proposition will show examples where locally stability is not satisfied, depending on how S and $\mathrm{supp}(Q)$ are specified, and it should be obvious to the reader that local stability will not be satisfied in many other cases as well. We let $\epsilon = \inf \mathrm{supp}(Q)$ and $R = \sup \mathrm{supp}(Q)$.

Proposition 7. *Local stability is satisfied for*

(a) the A-interaction process if and only if $\theta_1 \leq 0$ or $R < \infty$;

(b) the L-interaction process if $\theta_2 = 0$, or $R < \infty$ if $\theta_2 > 0$, or $\epsilon > 0$ and $R < \infty$ if $\theta_2 < 0$; otherwise in general it is not locally stable;

(c) the χ-interaction process if $\theta_3 \geq 0$, while in general it is not locally stable if $\theta_3 < 0$;

(d) the N_{cc}-interaction process if $\theta_3 = \theta_4 \geq 0$ or both $\theta_3 = \theta_4 < 0$ and $\epsilon > 0$, while it is not locally stable if $\theta_3 = \theta_4 < 0$ and $\epsilon = 0$;

(e) the N_{ic}-interaction process if $\theta_5 \geq 0$ or $\epsilon > 0$, while it is not locally stable if $\theta_5 < 0$ and $\epsilon = 0$.

Moreover, local stability is in general not satisfied for

(f) the N_{h}-interaction process unless $\theta_4 = 0$;

(g) the N_{bv}-interaction process unless $\theta_6 = 0$.

Proof. Let $\mathbf{x} \in \mathcal{N}$ and $v \in \Omega \setminus \mathbf{x}$.

It follows from (11) that $\lambda_{\theta_1}(\emptyset, v) = \exp\left(\pi\theta_1 r^2\right)$, $\lambda_{\theta_1}(\mathbf{x}, v) \leq \exp\left(\pi\theta_1 r^2\right)$ if $\theta_1 \geq 0$, and $\lambda_{\theta_1}(\mathbf{x}, v) \leq 1$ if $\theta_1 \leq 0$. Thereby (a) follows, and in a similar way we verify (b)

in the case $\theta_2 \geq 0$. It also follows from (11) that the χ-interaction process is locally stable if $\theta_3 \geq 0$.

To verify (b) in the case $\theta_2 < 0$, we suppose first that $\epsilon > 0$ and $R < \infty$, and use an argument which Wilfrid Kendall kindly has point out to us. A boundary edge corresponding to an angle $0 < \varphi < 2\pi$ and a disc of radius r has length φr, and it defines a sector of area $\varphi r^2/2$. Since such sectors have disjoint interiors,

$$A(\mathcal{U}_{\mathbf{x}}) \geq \sum_j \varphi_j r_j^2/2 \geq (\epsilon^2/2) \sum_j \varphi_j$$

where the sum is over all boundary edges. Hence

$$L(\mathcal{U}_{\mathbf{x}}) = \sum_j \varphi_j r_j \leq R \sum_j \varphi_j \leq (2R/\epsilon^2) A(\mathcal{U}_{\mathbf{x}}) < c$$

where c is a finite constant (since the discs specified by $\mathbf{x}$ have centres in the bounded region S and their radii are bounded by R, $A(\mathcal{U}_{\mathbf{x}})$ has an upper bound). Consequently,

$$L(\mathbf{x}, v) = L(b_v) - L(b_v \cap \mathcal{U}_{\mathbf{x}}) \geq 2\pi\epsilon - c$$

and so local stability is established when $\theta_2 < 0$, $\epsilon > 0$, and $R < \infty$.

On the other hand, suppose that $\epsilon = 0$ or $R = \infty$. Let r denote the radius of b_v, let $0 < \delta < r$, and consider the infinite configuration of discs of radii δ and centres at the sites of a equilateral triangular lattice of side length 2δ. The proportion of $\mathbb{R}^2$ covered by these discs is the so-called maximal packing degree $p = \pi/\sqrt{12}$ (a number independent on how δ is chosen). Now, suppose that $\mathbf{x}$ is the subconfiguration of all such discs contained in b_v. As either δ decreases to zero or r increases to infinity, $n(\mathbf{x})\delta^2/r^2$ converges to p, and so

$$L(\mathbf{x}, v) = L(b_v) - L(b_v \cap \mathcal{U}_{\mathbf{x}}) = 2\pi r - 2\pi\delta n(\mathbf{x})$$

is converging to $-\infty$. Hence if $\theta_2 < 0$, the local stability condition is violated, and so (b) is verified.

To show an example where the χ-interaction process is not locally stable if $\theta_3 < 0$, consider Figure 12. Suppose $\mathbf{x} = \{x_1, \ldots, x_n\}$ corresponds to the pairwise overlapping small discs in the figure, and b_v to the large disc. Then each pair x_i, x_{i+1} together with b_v form one hole, and $N_{\mathrm{h}}(b_v \cap \mathcal{U}_{\mathbf{x}}) = n - 1$. Since n may be arbitrary large, using

again (11), we obtain (c). Notice that b_v does not need to be so large compared to the other discs in Figure 12; it is only chosen in this way for illustrative purposes. For example, all the discs may be of a very similar size so that still $N_{\mathrm{h}}(b_v \cap \mathcal{U}_{\mathbf{x}}) = n - 1$ (then the discs in $\mathbf{x}$ will be much more overlapping than indicated in Figure 12). More precisely, whether this holds or not depends on how large S is compared to $\mathrm{supp}(Q)$. For instance, if S is a disc with radius R and $\Omega = S \times \{2R\}$, then $\chi(\mathcal{U}_{\mathbf{x}}) = 1$ for all $\mathbf{x} \in \mathcal{N}$, and so the χ-interaction process is locally stable for all $\theta_3 \in \mathbb{R}$.

For (d), we use that

$$N_{\mathrm{cc}}(\mathbf{x}, v) = 1 - \#\{\text{connected components in } \mathcal{U}_{\mathbf{x}} \text{ which are intersected by } b_v\}. \quad (33)$$

Hence we immediately obtain local stability if $\theta_3 = \theta_4 \geq 0$. Suppose instead that $\theta_3 = \theta_4 < 0$. By (33), $N_{\mathrm{cc}}(\mathbf{x}, v)$ has no lower bound if $\epsilon = 0$, since the discs in $\mathbf{x}$ can be disjoint and still all intersect b_v. On the other hand, if $\epsilon > 0$, then $1 - N_{\mathrm{cc}}(\mathbf{x}, v)$ is at most equal to the maximal number of disjoint discs with radius ϵ and centres in S. Thereby (d) is verified. The proof of (e) is similar, using instead that

$$N_{\mathrm{ic}}(\mathbf{x}, v) = \mathbf{1}_{\mathrm{ic}}(\mathbf{x}, v) - \#\{\text{isolated cells in } \mathcal{U}_{\mathbf{x}} \text{ which are contained in } b_v\}$$

where $\mathbf{1}_{\mathrm{ic}}(\mathbf{x}, v)$ is the indicator function which is one if B_v is an isolated cell in $\mathcal{B}_{\mathbf{x} \cup \{v\}}$, and zero otherwise.

The N_{h}-interaction process with $\theta_4 = 0$ and the N_{bv}-interaction process with $\theta_6 = 0$ are nothing but the Poisson process $\mathbf{\Psi}$, and so local stability is obviously satisfied. By similar arguments as above in the proof of (c) when $\theta_3 < 0$, there are in general no uniform upper and lower bounds on neither $N_{\mathrm{h}}(\mathbf{x}, v)$ nor $N_{\mathrm{bv}}(\mathbf{x}, v)$. Thereby (f) and (g) follow.

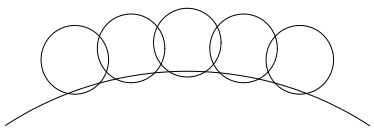

FIGURE 12: A configuration $\mathbf{x}$ of $n = 6$ discs intersected by another disc b_v such that $\#\mathrm{holes}(b_v \cap \mathcal{U}_{\mathbf{x}}) = n - 1 = 5$.

Proposition 7 immediately extends to the conditional quarmass-interaction process with density (28) and the conditional T-interaction process in (30). Note that if the indicator term in (30) is one, it implies that the radius of any disc in $\mathbf{x}^{(a)}$ is less than a constant. Consequently, (a) the conditional A-interaction process given by (30) is always locally stable, and (b) the L-interaction process given by (30) is locally stable if either $\theta_2 \geq 0$ or $\theta_2 < 0$ and $\epsilon > 0$, and in general it is not locally stable if $\theta_2 < 0$ and $\epsilon = 0$.

4.7. MCMC algorithms

For simulation of the T-interaction process (6), the conditional quarmass-interaction point process with density (28), or the conditional T-interaction process with density (30), we use a simple version of the birth-death type Metropolis-Hastings algorithm studied in [13, 14, 33]. For specificity, we consider first the T-interaction process $\mathbf{X}$ with Papangelou conditional intensity $\lambda_\theta(\mathbf{x}, v)$ given by (8).

In the Metropolis-Hastings algorithm, if $\mathbf{x}$ is the state at iteration t, we generate a proposal which is either a 'birth' $\mathbf{x} \cup \{v\}$ of a new discs $v = (z, r)$ or a 'death' $\mathbf{x} \setminus \{x_i\}$ of an old disc $x_i \in \mathbf{x}$. Each kind of proposal may happen with equal probability 1/2. Define

$$r_\theta(\mathbf{x}, v) = \lambda_\theta(\mathbf{x}, v) \frac{\int_S \rho(s)\,\mathrm{d}s}{\rho(z)(n(\mathbf{x}) + 1)}. \tag{34}$$

In case of a birth-proposal, v follows the normalized intensity measure of $\mathbf{\Psi}$, i.e. z and r are independent, z has a density on S proportional to ρ, and r follows the mark distribution Q. This proposal is accepted as the state at iteration $t+1$ with probability $\min\{1, H_\theta(\mathbf{x}, v)\}$, where the Hastings ratio is given by $H_\theta(\mathbf{x}, v) = r_\theta(\mathbf{x}, v)$. In case of a death-proposal, x_i is a uniformly selected point from $\mathbf{x}$, and the Hastings ratio in the acceptance probability of the proposal is now given by $H_\theta(\mathbf{x}, x_i) = 1/r_\theta(\mathbf{x} \setminus \{x_i\}, x_i)$ (in the special case where $\mathbf{x} = \emptyset$, we do nothing). Finally, if neither kind of proposal is accepted, we retain $\mathbf{x}$ at iteration $t + 1$.

As verified in [14], the generated Markov chain is aperiodic and positive Harris recurrent, the chain converges towards the distribution of $\mathbf{X}$, and Birkhoff's ergodic theorem establishes convergence of Monte Carlo estimates of mean values with respect to (6). If local stability is satisfied (see Proposition 7), the chain is geometrical ergodic, and hence a central limit theorem applies for Monte Carlo estimates [6, 33, 38].

Moreover, from a computational perspective, the important point of the algorithm is that it only involves calculating the Papangelou conditional intensity, so only local computations of the statistics appearing in (8) are needed, cf. Sections 4.3-4.5.

In theory we may use any state of $\mathcal{N}$ as the initial state of the algorithm, but we have mainly used three kinds of initial states:

(i) the extreme case of the empty configuration $\emptyset$;

(ii) if local stability is satisfied, the other extreme case is given by a realization from a Poisson process $\boldsymbol{\Xi}$ with intensity measure $\beta\rho(z)\,\mathrm{d}z\,Q(\mathrm{d}r)$, where β is the upper bound in (32);

(iii) a realization of the reference Poisson process $\boldsymbol{\Psi}$ (an intermediate case of (i)-(ii) if $\beta > 1$).

In fact local stability ensures that the Poisson process in (ii) can be coupled with $\mathbf{X}$ so that $\mathbf{X} \subseteq \boldsymbol{\Xi}$, and this kind of domination can be exploited to make perfect simulations of $\mathbf{X}$, using a dominating coupling from the past algorithm [21, 22].

The algorithm for simulating from the conditional processes with densities (28) and (30) is the same except that we replace $\lambda_\theta(\mathbf{x}, v)$ in (34) by the Papangelou conditional intensities in (29)-(31), and that the state space has of course to be in accordance with (28) respective (30). The convergence properties and computations are therefore similar to those discussed above. The initial states are of course slightly different, where we modify the Poisson process in (ii) or (iii) above as follows. For (28), we restrict the Poisson process in (ii) or (iii) so that centres are in $W_{\ominus 2R}$. For (30), we first restrict the Poisson process in (ii) or (iii) so that centres are in W, and second when we make a simulation from this Poisson process, we finally omit those discs which are not included in $W \setminus V$.

5. Extensions and open problems

We conclude with some remarks on possible extensions of this work and on some open problems.

We demonstrated the usefulness of the power tessellation in connection to the T-interaction process (4), and argued why this model is best viewed as a connected

component Markov point process. For the specification of the sufficient statistic T, other geometric characteristics than those in (4) may be of interest to include, e.g. shape characteristic for the connected components K such as $A(K)/L(K)^2$. The power tessellation will also be a useful tool for such extensions, not least since local calculations can be done as discussed in Section 4.4.

We confined ourselves to the case of discs in $\mathbb{R}^2$, though many concepts and results can be extended to the general case of balls in $\mathbb{R}^d$. The planar case $d = 2$ is already complicated enough, and indeed the power tessellation in higher dimensions becomes more complicated, cf. [10]. The planar case is of principal importance for applications in spatial statistics and stochastic geometry (e.g. [8, 40]), and the spatial case $d = 3$ is of particular importance in physics and computational biology (e.g. [11, 24, 25, 26]).

The T-interaction processes provide obviously a large and flexible class of random models for unions of discs. It would be interesting to get a better understanding of the importance of the parameters $\theta_1, \ldots, \theta_6$, cf. Section 4.2. For instance, how different are the models which have been simulated in Section 4.2, and how different would a fitted L-interaction process be if the true model is an A-interaction process? Probably, to answer such questions, an extensive simulation study will be required.

As noticed in Section 4.6, the dominating coupling from the past algorithm [18, 22] for making perfect simulations requires local stability. Moreover, to make this algorithm work in practice, some monotonicity property like (9) or an antimonotonicity property like (10) is useful, but apart from the A-interaction process, our models are in general neither attractive nor repulsive, cf. Proposition 2. How difficult is it to make a perfect simulation of e.g. the L-interaction process?

Also extensions of our T-interaction models to infinite configurations of discs would be of interest, particularly for applications in statistical physics. Such extensions are possible for quarmass-interaction models, at least if Q has bounded support (see [19]), but how do we extend the other kind of T-interaction models? The usual approach is to use a local specification in the sense of Preston [36] or equivalently to specify the Papangelou conditional intensity for the infinite process [12, 34], but this would require that the connected components are almost surely bounded. See the somewhat related discussion in [32] concerning infinite extensions of Markov connected component fields.

A related problem to infinite extensions of T-interaction models is the issue of phase

transition. The A-interaction model exhibits phase transition, at least if the radii are all fixed at a constant value [15, 39], but what about other T-interaction models?

Finally, we are currently exploiting the results in this paper when studying the statistical aspects, in particular likelihood based inference, in a follow up paper [31].

Acknowledgements

We are grateful to Lars Døvling Andersen, Herbert Edelsbrunner, and Wilfrid Kendall for useful comments. Supported by the Danish Natural Science Research Council, grant 272-06-0442, "Point process modelling and statistical inference", and by grants GAČR 201/06/0302 and GAČR 201/05/H007.

Appendix: successive construction of power tessellations

This appendix explains how to construct a new power tessellation of a union of discs by adding a new ball (Appendix A) or deleting an old ball (Appendix B), assuming that the old power tessellation is known. The constructions can easily be extended to keep track on the connected components of the union of discs, but to save space we omit those details.

Appendix A: the case where a new disc is added

Suppose we want to construct a new power tessellation $\mathcal{B}^{\mathrm{new}}$ of a union $\mathcal{U}^{\mathrm{new}} = \cup_1^n b_i$ of $n \geq 1$ discs in general position, where we are adding the disc b_n and we have already constructed the power tessellation $\mathcal{B}^{\mathrm{old}}$ of $\mathcal{U}^{\mathrm{old}} = \cup_1^{n-1} b_i$ based on the $n-1$ other discs (if $n = 1$ then $\mathcal{B}^{\mathrm{old}}$ and $\mathcal{U}^{\mathrm{old}}$ are empty). More precisely, with respect to $\mathcal{B}^{\mathrm{old}}$, we assume to know all the old edges. We denote old interior edges by $[u_{i,j}^{\mathrm{old}}, v_{i,j}^{\mathrm{old}}]$ and old boundary edges by $\rfloor u_i^{\mathrm{old}}, v_i^{\mathrm{old}} \lceil$ or $\partial b_i^{\mathrm{old}}$. We want to construct the new tessellation $\mathcal{B}^{\mathrm{new}}$ of $\mathcal{U}^{\mathrm{new}} = \mathcal{U}^{\mathrm{old}} \cup b_n$ by finding its interior edges $[u_{i,n}^{\mathrm{new}}, v_{i,n}^{\mathrm{new}}]$ and boundary edges $\rfloor u_n^{\mathrm{new}}, v_n^{\mathrm{new}} \lceil$ associated to the new cell B_n^{new}. This is done in steps (ii) and (iv) below. Moreover, to obtain the remaining new edges, we modify old interior edges $[u_{i,j}^{\mathrm{old}}, v_{i,j}^{\mathrm{old}}]$ and old boundary edges $\rfloor u_i^{\mathrm{old}}, v_i^{\mathrm{old}} \lceil$ or $\partial b_i^{\mathrm{old}}$, noticing that a "modified old edge" can be unchanged, reduced or disappearing. This is done in steps (iii) and (v) below. Notice that steps (i), (ii), and (iv) determine the new cells, i.e. which of the sets

$B_1^{\rm new}, \ldots, B_n^{\rm new}$ are empty or not.

(i) Considering old discs intersecting the new disc: If b_n is contained in some disc b_j with $j < n$, then $B_n^{\rm new}$ is empty and so $\mathcal{B}^{\rm new} = \mathcal{B}^{\rm old}$ is unchanged. Assume that b_n is not contained in any disc b_j with $j < n$, and without loss of generality that b_n intersects $B_1^{\rm old}, \ldots, B_i^{\rm old}$ but not $B_{i+1}^{\rm old}, \ldots, B_{n-1}^{\rm old}$, where $0 \leq i \leq n-1$ (setting $i = 0$ if b_n has no intersection). Then $B_j^{\rm new} = B_j^{\rm old}$ is unchanged for $j = i+1, \ldots, n-1$, so it suffices below to find the edges of $B_1^{\rm new}, \ldots, B_i^{\rm new}$ and $B_n^{\rm new}$.

If $i = 0$ then $B_n^{\rm new} = b_n$ is an isolated cell with boundary edge ∂b_n. In (ii)-(v) we assume that $i \geq 1$.

(ii) Finding the interior edges of $B_n^{\rm new}$: To obtain the interior edges of $B_n^{\rm new}$, for $j = 1, \ldots, i$, we start by assigning $e_{j,n}^{\rm new} \leftarrow [u_{j,n}^{\rm new}, v_{j,n}^{\rm new}]$, considering $u_{j,n}^{\rm new}$ and $v_{j,n}^{\rm new}$ as (potential) boundary vertices given by the endpoints of the chord $E_{j,n}$. Further, for $k = 1, \ldots, i$ with $k \neq j$, if $e_{j,n}^{\rm new} \cap H_{n,k} = \emptyset$ (or equivalently $u_{j,n}^{\rm new} \notin H_{n,k}$ and $v_{j,n}^{\rm new} \notin H_{n,k}$, since $H_{n,k}$ is convex) we obtain that $e_{j,n}^{\rm new} \leftarrow \emptyset$ and we can stop the k-loop, else $e_{j,n}^{\rm new} \leftarrow e_{j,n}^{\rm new} \cap H_{n,k}$. In the latter case, either both vertices are contained in $H_{n,k}$ and so the edge remains unchanged, or exactly one vertex is not contained in $H_{n,k}$, e.g. $u_{j,n}^{\rm new} \notin H_{n,k}$ but $v_{j,n}^{\rm new} \in H_{n,k}$, in which case $u_{j,n}^{\rm new}$ becomes an interior vertex given by the point $e_{j,n}^{\rm new} \cap \partial H_{n,k}$ while $v_{j,n}^{\rm new}$ is unchanged. In this way we find all interior edges of $B_n^{\rm new}$, and all interior and boundary vertices of $B_n^{\rm new}$.

Since we have assumed that $i > 0$, $B_n^{\rm new}$ is empty if and only if it has no interior edges.

(iii) Modifying the old interior edges: At the same time as we do step (ii) above, we also check whether each interior edge $e_{j,k}^{\rm old} = [u_{j,k}^{\rm old}, v_{j,k}^{\rm old}]$ of $\mathcal{B}^{\rm old}$ with $j < k \leq i$ should be kept, reduced or omitted when we consider $\mathcal{B}^{\rm new}$ (recalling that $e_{j,k}^{\rm new} = e_{j,k}^{\rm old}$ is unchanged if $j > i$ or $k > i$). We have

$$e_{j,k}^{\rm new} = e_{j,k}^{\rm old} \cap H_{j,n} = e_{j,k}^{\rm old} \cap H_{k,n}.$$

Thus $e_{j,k}^{\rm new}$ is empty if $u_{j,k}^{\rm old} \notin H_{k,n}$ and $v_{j,k}^{\rm old} \notin H_{k,n}$, while $e_{j,k}^{\rm new} = e_{j,k}^{\rm old}$ if $u_{j,k}^{\rm old} \in H_{k,n}$ and $v_{j,k}^{\rm old} \in H_{k,n}$. Further, if $u_{j,k}^{\rm old} \in H_{k,n}$ and $v_{j,k}^{\rm old} \notin H_{k,n}$, then $e_{j,k}^{\rm new} = [u_{j,k}^{\rm old}, v_{j,k}^{\rm new}]$ where $v_{j,k}^{\rm new}$ is the point given by $e_{j,k}^{\rm old} \cap \partial H_{k,n}$. Similarly, if $u_{j,k}^{\rm old} \notin H_{k,n}$ and $v_{j,k}^{\rm old} \in H_{k,n}$, then $e_{j,k}^{\rm new} = [u_{j,k}^{\rm new}, v_{j,k}^{\rm old}]$ where $u_{j,k}^{\rm new}$ is the point given by $e_{j,k}^{\rm old} \cap \partial H_{k,n}$.

Note that for each $j \leq i$, $B_j^{\rm new}$ is empty if and only if it has no interior edge.

(iv) Finding the boundary edges of B_n^{new}: Suppose that B_n^{new} has $m > 0$ boundary vertices $w_1^{\text{new}}, \ldots, w_m^{\text{new}}$. Notice that m is an even number, and we can organize the boundary vertices such that $w_1^{\text{new}} = z_n + r_n(\cos\varphi_1^{\text{new}}, \sin\varphi_1^{\text{new}})$, ..., $w_m^{\text{new}} = z_n + r_n(\cos\varphi_m^{\text{new}}, \sin\varphi_m^{\text{new}})$, where $0 \le \varphi_1^{\text{new}} < \cdots < \varphi_m^{\text{new}} < 2\pi$. Then B_n^{new} has $m/2$ boundary edges, namely

$$\lfloor w_2^{\text{new}}, w_3^{\text{new}}\rceil, \lfloor w_4^{\text{new}}, w_5^{\text{new}}\rceil, \ldots, \lfloor w_m^{\text{new}}, w_1^{\text{new}}\rceil \quad \text{if } z_n + (r_n, 0) \in H_{n,j} \text{ for all } j = 1, \ldots, i$$

and

$$\lfloor w_1^{\text{new}}, w_2^{\text{new}}\rceil, \lfloor w_3^{\text{new}}, w_4^{\text{new}}\rceil, \ldots, \lfloor w_{m-1}^{\text{new}}, w_m^{\text{new}}\rceil \quad \text{otherwise.}$$

(v) Modifying the old boundary edges: Finally, we modify the boundary edges $\lfloor u_j^{\text{old}}, v_j^{\text{old}}\rceil$ of $\mathcal{B}^{\text{old}}$ considering $\mathcal{B}^{\text{new}}$ and $j \le i$ (noticing that $\lfloor u_j^{\text{old}}, v_j^{\text{old}}\rceil$ is a boundary edge of $\mathcal{B}^{\text{new}}$ too if $j > i$). This is done in a similar way as in step (iv). Suppose that B_j^{new} has $m_j > 0$ boundary vertices $w_1^{\text{new}}, \ldots, w_{m_j}^{\text{new}}$, which we organize as in (iv). Then B_j^{new} has boundary edges

$$\lfloor w_2^{\text{new}}, w_3^{\text{new}}\rceil, \lfloor w_4^{\text{new}}, w_5^{\text{new}}\rceil, \ldots, \lfloor w_{m_j}^{\text{new}}, w_1^{\text{new}}\rceil$$
$$\text{if } z_j + (r_j, 0) \in H_{j,k} \text{ for all } k \le n \text{ with } k \ne j \text{ and } b_j \cap b_k \ne \emptyset$$

and

$$\lfloor w_1^{\text{new}}, w_2^{\text{new}}\rceil, \lfloor w_3^{\text{new}}, w_4^{\text{new}}\rceil, \ldots, \lfloor w_{m_{j-1}}^{\text{new}}, w_{m_j}^{\text{new}}\rceil \quad \text{otherwise.}$$

Appendix B: the case where a disc is deleted

Suppose we are deleting the disc b_n from a configuration $\{b_1, \ldots, b_n\}$ of $n \ge 1$ discs, which are assumed to be in general position. We also assume that we know the power tessellation $\mathcal{B}^{\text{old}}$ of $\mathcal{U}^{\text{old}} = \cup_1^n b_i$. Below we explain how to construct the new power tessellation $\mathcal{B}^{\text{new}}$ of $\mathcal{U}^{\text{new}} = \cup_1^{n-1} b_i$. More precisely, with respect to $\mathcal{B}^{\text{old}}$, we assume to know all the interior edges $[u_{i,j}^{\text{old}}, v_{i,j}^{\text{old}}]$ and all the boundary edges $\lfloor u_i^{\text{old}}, v_i^{\text{old}}\rceil$. We want to construct the tessellation $\mathcal{B}^{\text{new}}$ of $\mathcal{U}^{\text{new}} = \mathcal{U}^{\text{old}} \setminus b_n$ by finding the interior edges $[u_{i,j}^{\text{new}}, v_{i,j}^{\text{new}}]$ and the boundary edges $\lfloor u_i^{\text{new}}, v_i^{\text{new}}\rceil$ associated to each new cell B_i^{new}, noticing that B_i^{new} either agrees with B_i^{old} or is an enlargement of B_i^{old} or is a completely new cell. One possibility could be to "reverse" the construction in Appendix A, where a new disc is added, however, we realized that it is easier to create the new edges without reversing the construction in Appendix A but using a

construction as described below. This is partly explained by the fact that an old empty set B_i^{old} may possibly be replaced by a non-empty set B_i^{new}.

(i) Considering the discs intersecting the disc which is deleted: Clearly, if B_n^{old} is empty, then $\mathcal{B}^{\mathrm{new}} = \mathcal{B}^{\mathrm{old}}$ is unchanged. Assume that B_n^{old} is a non-empty cell, and without loss of generality that b_n intersects $b_1, \ldots, b_i$ but not $b_{i+1}, \ldots, b_{n-1}$, where $0 \leq i \leq n-1$ (setting $i = 0$ if b_n has no intersection). Then it suffices to find the edges of $B_1^{\mathrm{new}}, \ldots, B_i^{\mathrm{new}}$, since $B_j^{\mathrm{new}} = B_j^{\mathrm{old}}$ is unchanged for $j = i+1, \ldots, n-1$. If $i = 0$ then $B_n^{\mathrm{old}} = b_n$ is an isolated cell, and so $B_1^{\mathrm{new}} = B_1^{\mathrm{old}}, \ldots, B_{n-1}^{\mathrm{new}} = B_{n-1}^{\mathrm{old}}$ are unchanged. In the following steps (ii)-(iv), suppose that $i > 0$.

(ii) Finding the new interior edges: If $i = 1$, no new interior edge appears. Suppose that $i \geq 2$. We want to determine each set $e_{j,k}^{\mathrm{new}}$ with $j < k \leq i$. We start by assigning all cells $B_1^{\mathrm{new}}, \ldots, B_i^{\mathrm{new}}$ to be non-empty, and by assigning $e_{j,k}^{\mathrm{new}} \leftarrow [u_{j,k}^{\mathrm{new}}, v_{j,k}^{\mathrm{new}}]$, considering $u_{j,k}^{\mathrm{new}}$ and $v_{j,k}^{\mathrm{new}}$ as (potential) boundary vertices given by the endpoints of the chord $E_{j,k}$. Consider a loop with $l = 1, \ldots, i$ and $l \neq j, k$. If $e_{j,k}^{\mathrm{new}} \cap H_{k,l} = \emptyset$ (or equivalently $u_{j,k}^{\mathrm{new}} \notin H_{k,l}$ and $v_{j,k}^{\mathrm{new}} \notin H_{k,l}$, since $H_{k,l}$ is convex), we have that $e_{j,k}^{\mathrm{new}}$ is empty and we can stop the l-loop. Otherwise assign $e_{j,k}^{\mathrm{new}} \leftarrow e_{j,k}^{\mathrm{new}} \cap H_{k,l}$, where we notice that only the following two cases can occur. First, if both vertices of $e_{j,k}^{\mathrm{new}}$ are contained in $H_{k,l}$, the edge remains unchanged. Second, if exactly one vertex is not contained in $H_{k,l}$, e.g. $u_{j,k}^{\mathrm{new}} \notin H_{k,l}$ but $v_{j,k}^{\mathrm{new}} \in H_{k,l}$, then $u_{j,k}^{\mathrm{new}}$ becomes an interior vertex given by the point $e_{j,k}^{\mathrm{new}} \cap \partial H_{k,l}$ while $v_{j,k}^{\mathrm{new}}$ is unchanged. When the loop is finished, we have determined all the new interior edges, including the information whether their endpoints are interior or boundary vertices.

(iii) Determining the new cells: For each $j \leq i$, we determine if B_j^{new} is a new cell by checking if it has an edge. Suppose that B_j^{new} has no interior edge, i.e. it is either an empty set or a new isolated cell. If an arbitrary fixed point of b_j is included in $H_{j,l}$ for all $l = 1, \ldots, n-1$ with $l \neq j$, then B_j has exactly one boundary edge and it is an isolated cell. Otherwise B_j^{new} is empty. In this way we determine whether each B_j^{new} is empty or a new cell, including whether it is an isolated cell.

(iv) Finding the new boundary edges: We have already determined the new isolated boundary edges in step (iii). Consider a non-isolated cell B_j^{new} with $j \leq i$ with boundary vertices $w_k^{\mathrm{new}} = z_j + r_j(\cos\varphi_k^{\mathrm{new}}, \sin\varphi_k^{\mathrm{new}})$, $k = 1, \ldots, m_j$. Recall that $m_j > 0$ is an even number and we organize the vertices so that $0 \leq \varphi_1^{\mathrm{new}} < \cdots < \varphi_{m_j}^{\mathrm{new}} < 2\pi$,

cf. (iv) in Appendix A. Then B_j^{new} has $m_j/2$ boundary edges, namely

$$\lfloor w_2^{\mathrm{new}}, w_3^{\mathrm{new}} \rceil, \lfloor w_4^{\mathrm{new}}, w_5^{\mathrm{new}} \rceil, \ldots, \lfloor w_{m_j}^{\mathrm{new}}, w_1^{\mathrm{new}} \rceil \quad \text{if } z_j + (r_j, 0) \in H_{j,l} \text{ for all } l = 1, \ldots, i$$

and

$$\lfloor w_1^{\mathrm{new}}, w_2^{\mathrm{new}} \rceil, \lfloor w_3^{\mathrm{new}}, w_4^{\mathrm{new}} \rceil, \ldots, \lfloor w_{m_j-1}^{\mathrm{new}}, w_{m_j}^{\mathrm{new}} \rceil \quad \text{otherwise.}$$

References

[1] Aurenhammer, F. (1987). Power diagrams: properties, algorithms and applications. *SIAM Journal on Computing* **16,** 78–96.

[2] Baddeley, A. and Møller, J. (1989). Nearest-neighbour Markov point processes and random sets. *International Statistical Review* **2,** 89–121.

[3] Baddeley, A. J. and van Lieshout, M. N. M. (1995). Area-interaction point processes. *Annals of the Institute of Statistical Mathematics* **46,** 601–619.

[4] Baddeley, A. J., van Lieshout, M. N. M. and Møller, J. (1996). Markov properties of cluster processes. *Advances in Applied Probability* **28,** 346–355.

[5] Barndorff-Nielsen, O. E. (1978). *Information and Exponential Families in Statistical Theory.* Wiley, Chichester.

[6] Chan, K. S. and Geyer, C. J. (1994). Discussion of the paper 'Markov chains for exploring posterior distributions' by Luke Tierney. *Annals of Statistics* **22,** 1747–1747.

[7] Chin, Y. C. and Baddeley, A. J. (2000). Markov interacting component processes. *Advances in Applied Probability* **32,** 597–619.

[8] Cressie, N. A. C. (1993). *Statistics for Spatial Data* second ed. Wiley, New York.

[9] Diggle, P. (1981). Binary mosaics and the spatial pattern of heather. *Biometrics* **37,** 531–539.

[10] Edelsbrunner, H. (1995). The union of balls and its dual shape. *Discrete Computational Geometry* **13,** 415–440.

[11] Edelsbrunner, H. (2004). Biological applications of computational topology. In *Handbook of Discrete and Computational Geometry*. ed. J. Goodman and J. O'Rourke. Chapman and Hall/CRC, Boca Raton pp. 1395–1412.

[12] Georgii, H.-O. (1976). Canonical and grand canonical Gibbs states for continuum systems. *Communications of Mathematical Physics* **48,** 31–51.

[13] Geyer, C. J. (1999). Likelihood inference for spatial point processes. In *Stochastic Geometry: Likelihood and Computation*. ed. O. E. Barndorff-Nielsen, W. S. Kendall, and M. N. M. van Lieshout. Chapman & Hall/CRC, Boca Raton, Florida. pp. 79–140.

[14] Geyer, C. J. and Møller, J. (1994). Simulation procedures and likelihood inference for spatial point processes. *Scandinavian Journal of Statistics* **21,** 359–373.

[15] Häggström, O., van Lieshout, M. N. M. and Møller, J. (1999). Characterization results and Markov chain Monte Carlo algorithms including exact simulation for some spatial point processes. *Bernoulli* **5,** 641–659.

[16] Hall, P. (1988). *Introduction to the Theory of Coverage Processes*. Wiley, New York.

[17] Hanisch, K.-H. (1981). On classes of random sets and point processes. *Serdica* **7,** 160–167.

[18] Kendall, W. (2004). Geometric ergodicity and perfect simulation. *Electronic Communications in Probability* **9,** 140–151.

[19] Kendall, W., van Lieshout, M. and Baddeley, A. (1999). Quermass-interaction processes: conditions for stability. *Advances in Applied Probability* **31,** 315–342.

[20] Kendall, W. S. (1990). A spatial Markov property for nearest-neighbour Markov point processes. *Journal of Applied Probability* **28,** 767–778.

[21] Kendall, W. S. (1998). Perfect simulation for the area-interaction point process. In *Probability Towards 2000*. ed. L. Accardi and C. Heyde. Springer Lecture Notes in Statistics 128, Springer Verlag, New York pp. 218–234.

[22] Kendall, W. S. and Møller, J. (2000). Perfect simulation using dominating processes on ordered spaces, with application to locally stable point processes. *Advances in Applied Probability* **32,** 844–865.

[23] Klein, W. (1982). Potts-model formulation of continuum percolation. *Physical Review B* **26,** 2677–2678.

[24] Likos, C., Mecke, K. and Wagner, H. (1995). Statistical morphological of random interfaces in microemulsions. *Journal of Chemical Physics* **102,** 9350–9361.

[25] Mecke, K. (1994). *Integralgeometrie in der Statistichen Physik*. Reine Physik Volume 25, Harri Deutsch, Frankfurt.

[26] Mecke, K. (1996). A morphological model for complex fluids. *Journal of Physics: Condensed Matters* **8,** 9663–9667.

[27] Molchanov, I. (1997). *Statistics of the Boolean Model for Practitioners and Mathematicians*. Wiley, Chichester.

[28] Møller, J. (1994). Contribution to the discussion of N.L. Hjort and H. Omre (1994): Topics in spatial statistics. *Scandinavian Journal of Statistics* **21,** 346–349.

[29] Møller, J. (1994). *Lectures on Random Voronoi Tessellations*. Lecture Notes in Statistics 87. Springer-Verlag, New York.

[30] Møller, J. (1999). Markov chain Monte Carlo and spatial point processes. In *Stochastic Geometry: Likelihood and Computation*. ed. O. E. Barndorff-Nielsen, W. S. Kendall, and M. N. M. van Lieshout. Monographs on Statistics and Applied Probability 80, Chapman & Hall/CRC, Boca Raton, Florida pp. 141–172.

[31] Møller, J. and Helisová, K. (2007). Likelihood inference for unions of interacting discs. In preparation.

[32] Møller, J. and Waagepetersen, R. P. (1998). Markov connected component fields. *Advances in Applied Probability* **30,** 1–35.

[33] Møller, J. and Waagepetersen, R. P. (2003). *Statistical Inference and Simulation for Spatial Point Processes.* Chapman and Hall/CRC, Boca Raton.

[34] Nguyen, X. X. and Zessin, H. (1979). Integral and differential characterizations of Gibbs processes. *Mathematische Nachrichten* **88,** 105–115.

[35] Okabe, A., Boots, B., Sugihara, K. and Chiu, S. N. (2000). *Spatial Tessellations. Concepts and Applications of Voronoi Diagrams* second ed. Wiley, Chichester.

[36] Preston, C. J. (1977). Spatial birth-and-death processes. *Bulletin of the International Statistical Institute* **46,** 371–391.

[37] Ripley, B. D. and Kelly, F. P. (1977). Markov point processes. *Journal of the London Mathematical Society* **15,** 188–192.

[38] Roberts, G. O. and Rosenthal, J. S. (1997). Geometric ergodicity and hybrid Markov chains. *Electronic Communications in Probability* **2,** 13–25.

[39] Ruelle, D. (1971). Existence of a phase transition in a continuous classsical system. *Physical Review Letters* **27,** 1040–1041.

[40] Stoyan, D., Kendall, W. S. and Mecke, J. (1995). *Stochastic Geometry and Its Applications* second ed. Wiley, Chichester.

[41] Weil, W. and Wieacker, J. (1984). Densities for stationary random sets and point processes. *Advances in Applied Probability* **16,** 324–346.

[42] Weil, W. and Wieacker, J. (1988). A representation theorem for random sets. *Probability and Mathematical Statistics* **9,** 147–151.

[43] Widom, B. and Rowlinson, J. S. (1970). A new model for the study of liquid-vapor phase transitions. *Journal of Chemical Physics* **52,** 1670–1684.

[44] Wilson, R. (1972). *Introduction to Graph Theory.* Oliver and Boyd, Edinburgh.